Direct and Two-Step Positioning in Visible Light Systems

Musa Furkan Keskin, Sinan Gezici, and Orhan Arikan

***Abstract*—Visible light positioning (VLP) systems based on light emitting diodes (LEDs) can facilitate high accuracy localization services for indoor scenarios. In this study, direct and two-step positioning approaches are investigated for both synchronous and asynchronous VLP systems. First, the Cramér-Rao lower bound (CRLB) and the direct positioning based maximum likelihood (ML) estimator are derived for three-dimensional localization of a visible light communication (VLC) receiver in a synchronous scenario by utilizing information from both time delay parameters and channel attenuation factors. Then, a two-step position estimator is designed for synchronous VLP systems by exploiting the asymptotic properties of time-of-arrival (TOA) and received signal strength (RSS) estimates. The proposed two-step estimator is shown to be asymptotically optimal, i.e., converges to the direct estimator at high signal-to-noise ratios (SNRs). In addition, the CRLB and the direct and two-step estimators are obtained for positioning in asynchronous VLP systems. It is proved that the two-step position estimation is optimal in asynchronous VLP systems for practical pulse shapes. Various numerical examples are provided to illustrate the improved performance of the proposed estimators with respect to the current state-of-the-art and to investigate their robustness against model uncertainties in VLP systems.**

***Index Terms*– Estimation, Cramér-Rao lower bound, visible light, Lambertian pattern, direct positioning, two-step positioning.**

I. Introduction

A. Background and Motivation

Light emitting diode (LED) based visible light systems have found a widespread use for communication and localization in indoor environments due to the attractive property of simultaneous illumination, positioning, and high speed communications [1]–[12]. Unlike radio-frequency (RF) based indoor localization services, visible light positioning (VLP) systems can utilize an enormous unregulated visible light spectrum without suffering from interference due to RF communications [1], [2]. In addition, highly accurate localization performance has been obtained for VLP systems in the literature [13]–[18], which points out a viable opportunity for future applications.

Commonly, the problem of wireless localization is investigated by employing two classes of approaches, which are *two-step positioning* and *direct positioning*. Widely applied in RF and VLP based localization systems, two-step positioning algorithms extract position related parameters, such as received signal strength (RSS), time-of-arrival (TOA), time-difference-of-arrival (TDOA), and angle-of-arrival (AOA) in the first step, and perform position estimation based on those parameters in the second step [19]. There exist a multitude of applications of indoor VLP systems that employ two-step positioning, such as those using RSS [15], [18], [20], [21], AOA [9], hybrid RSS/AOA [22]–[24], TOA [5], [25], and TDOA [17]. However, the two-step method can be construed as a suboptimal solution to the localization problem since it does not exploit all the collected data related to the unknown location. On the other hand, direct positioning algorithms use the entire received signal in a one-step process in order to determine the unknown position, as opposed to two-step positioning [26]–[28]. Hence, all the available information regarding the unknown position can be effectively utilized in the direct position estimation approach, which can lead to the optimal solution to the localization problem. A theoretical justification for the superiority of direct positioning over conventional two-step positioning is provided in [29], [30]. In [26], the direct position determination (DPD) technique is proposed for localization of narrowband RF emitters, where the multiple signal classification (MUSIC) algorithm is employed to formulate the cost function in the case of unknown signals. It is shown that the DPD approach outperforms the conventional AOA based two-step localization technique. The study in [31] investigates the localization of a stationary narrowband RF source using signals from multiple moving receivers in a single-step approach and demonstrates that the DPD method is superior to the two-step differential Doppler (DD) method at low signal-to-noise ratios (SNRs). In addition, direct localization techniques are shown to enhance the performance of RF positioning in TOA [32], TDOA [33] and hybrid TOA/AOA [34] based systems. Direct positioning algorithms are also employed for target localization in radar systems [35], [36].

Although the DPD approach has been employed in numerous applications in RF localization systems, only a limited amount of research has been carried out on the utilization of DPD techniques in indoor VLP systems. In [37], RSS based VLP system with non-directional LEDs and a detector array consisting of multiple directional photo diodes (PDs) is proposed, where time-averaged RSS values at each PD are considered as the final observation for two-dimensional position estimation. In [38], which extends the study in [37], a correlation receiver is employed to obtain a single RSS estimate for each PD without optimizing for the correlator peak. However, from the direct positioning perspective, the proposed methods in [37] and [38] utilize only the time-averaged or correlation samples of the received signal, not the entire signal for localization. Furthermore, an asynchronous VLP system is designed in [39], where a Bayesian signal model is constructed to estimate the unknown position based on the entire received signal from multiple LEDs in the

M. F. Keskin, S. Gezici, and O. Arikan are with the Department of Electrical and Electronics Engineering, Bilkent University, 06800, Ankara, Turkey, Tel: +90-312-290-3139, Fax: +90-312-266-4192, Emails: {keskin,gezici,oarikan}@ee.bilkent.edu.tr.

Part of this work was presented at IEEE International Black Sea Conference on Communications and Networking (IEEE BlackSeaCom 2017)

presence of obstruction of signals from several LEDs.

To provide performance benchmarks for positioning algorithms, theoretical bounds on distance ('range') and position estimation in VLP systems have been considered in several studies in the literature [5], [6], [23], [25], [37], [40], [41]. The work in [6] derives the Cramér-Rao lower bound (CRLB) for distance estimation based on RSS information, whereas [5] presents the CRLB for distance estimation in synchronous visible light systems based on TOA measurements. The CRLB on hybrid TOA/RSS based ranging is investigated in [25]. In [40], the Ziv-Zakai bound (ZZB) is derived for synchronous VLP systems in the presence of prior information about distance and it is compared against the expected CRB (ECRB), Bayesian CRB (BCRB), and weighted CRB (WCRB), all of which utilize prior information. Besides distance estimation, theoretical accuracy limits have also been derived for localization in visible light systems. In [23], the CRLB is derived for RSS based three-dimensional localization for an indoor VLP scenario with arbitrary LED transmitter and visible light communication (VLC) receiver configurations. In [37] and [38], two-dimensional RSS-based localization is addressed with the assumption of a known receiver height, and an analytical CRLB expression is derived accordingly.

B. Contributions

In this manuscript, we investigate the fundamental limits of three-dimensional localization of a VLC receiver in synchronous and asynchronous VLP systems, design ML estimators by employing direct and two-step positioning techniques, and characterize the asymptotic performance of the proposed estimators via theoretical derivations. The main contributions of this manuscript can be summarized as follows:

- *Theoretical Bounds for Synchronous Scenarios:* For the first time in the literature, a general CRLB expression is derived for three-dimensional localization of a VLC receiver in synchronous VLP systems by utilizing information from both time delay parameters (i.e., TOA) and channel attenuation factors (i.e., RSS) (Proposition 1).
- *Algorithms/Estimators for Synchronous Scenarios:* The direct and two-step ML position estimators are proposed for synchronous VLP systems by taking into account both TOA and RSS information. The direct positioning approach, which exploits the whole observation signal, is considered for the first time for synchronous VLP systems. In addition, the two-step estimator is designed by exploiting the asymptotic properties of TOA and RSS estimates in the high SNR regime (Lemma 1). Moreover, it is shown that the proposed two-step estimator is *asymptotically optimal*, i.e., converges to the direct estimator at high SNRs (Proposition 2 and Remark 1).
- *Theoretical Bounds for Asynchronous Scenarios:* The CRLB for three-dimensional RSS-based localization is derived for asynchronous VLP systems (Proposition 3). The derived CRLB expression constitutes a generalization of that in [23] to cases in which transmitted pulses can have arbitrary shapes and LED transmission powers can have any values.
- *Algorithms/Estimators for Asynchronous Scenarios:* The ML estimators are designed for direct and two-step positioning in asynchronous VLP scenarios. It is proved that the two-step estimator is equivalent to the direct estimator for practical pulse shapes (Proposition 4). Hence, the two-step position estimation is shown to be optimal in the ML sense under practical conditions in asynchronous VLP systems.

The key differences between this work and the previous results on VLP systems can be listed as follows:

- *Theoretical Bounds:*
  - Different from the previous work on synchronous VLP systems (e.g., [5], [25], [40], [42]), which analyzes only distance estimation, this study investigates three-dimensional position estimation and puts forward a fundamental limit on the accuracy of localization in synchronous scenarios, which is valid for arbitrary transmitter/receiver positions and orientations.
  - Although there exist previous studies that focus on the CRLB derivation for localization in asynchronous VLP systems (e.g., [23], [37], [38]), theoretical bounds on localization in synchronous VLP systems are provided for the first time.
  - The analytical derivations are based *directly* on the received signal itself, not on measured/extracted quantities (as in, e.g., [23], [37], [38]), which leads to generalized expressions that can address scenarios with any type of transmitted signals.
- *Positioning Algorithms:*
  - Position estimators are proposed for generic three-dimensional VLP configurations. However, most of the existing work on positioning algorithms in VLP systems relies on the assumption of a known receiver height and/or perpendicular LED and VLC orientations (e.g., [7], [15], [18], [21], [43]), which can make those algorithms impractical in certain applications.
  - For asynchronous scenarios, different from the three-dimensional ML position estimator in [23], which is effectively a two-step estimator through the use of measured RSS values, we derive both the direct and the two-step estimators, and identify conditions under which these two positioning paradigms become equivalent.
  - As opposed to the previous VLP studies, we employ the optimal way of obtaining the RSS observations from the received signals via an ML approach (Section III-C and Section IV-B).
  - Regarding synchronous scenarios, to the best of authors' knowledge, there exist no previous studies in the literature that propose a positioning algorithm for synchronous VLP systems.

The rest of the manuscript is organized as follows: Section II presents the VLP system model. The CRLBs and the ML estimators are derived for synchronous and asynchronous systems in Section III and Section IV, respectively. Numerical

results are presented in Section V, and concluding remarks are provided in Section VI.

II. System Model

A. Received Signal Model

Consider a VLP system in which a number of LED transmitters are employed to estimate the position of a VLC receiver. A line-of-sight (LOS) scenario is assumed between each LED transmitter and the VLC receiver, which is commonly the case for visible light systems [4], [5]. Then, the received signal at the VLC receiver due to the signal emitted by the ith LED transmitter is formulated as [5]

$$r_i(t) = \alpha_i R_p \, s_i(t-\tau_i) + \eta_i(t) \tag{1}$$

for $i \in \{1,\dots,N_{\rm L}\}$ and $t \in [T_{1,i}, T_{2,i}]$, where $N_{\rm L}$ denotes the number of LED transmitters, $T_{1,i}$ and $T_{2,i}$ determine the observation interval for the signal coming from the ith LED transmitter, α_i is the attenuation factor of the optical channel between the ith LED transmitter and the VLC receiver ($\alpha_i > 0$), R_p is the responsivity of the photo detector, $s_i(t)$ is the transmitted signal from the ith LED transmitter, which is nonzero over an interval of $[0, T_{s,i}]$, τ_i is the TOA of the signal emitted by the ith LED transmitter, and $\eta_i(t)$ is zero-mean additive white Gaussian noise with spectral density level σ^2. It is assumed that a certain type of multiple access protocol, such as frequency-division or time-division multiple access [44], is employed in order to facilitate separate processing of signals from each LED transmitter at the VLC receiver [45]. Therefore, the noise processes corresponding to the received signals from different LED transmitters are modeled to be independent. It is also assumed that R_p and $s_i(t)$, $i \in \{1,\dots,N_{\rm L}\}$, are known by the VLC receiver.

The TOA parameter in (1) is modeled as

$$\tau_i = \frac{\|\boldsymbol{l}_{\rm r} - \boldsymbol{l}_{\rm t}^i\|}{c} + \Delta_i \tag{2}$$

where c is the speed of light, Δ_i denotes the time offset between the clocks of the ith LED transmitter and the VLC receiver, $\boldsymbol{l}_{\rm r} = [l_{{\rm r},1}\ l_{{\rm r},2}\ l_{{\rm r},3}]^T$ and $\boldsymbol{l}_{\rm t}^i = [l_{{\rm t},1}^i\ l_{{\rm t},2}^i\ l_{{\rm t},3}^i]^T$ are three-dimensional column vectors that denote the locations of the VLC receiver and the ith LED transmitter, respectively, and $\|\boldsymbol{l}_{\rm r} - \boldsymbol{l}_{\rm t}^i\|$ denotes the distance between the ith LED transmitter and the VLC receiver. For a synchronous scenario, $\Delta_i = 0$ for $i = 1,\dots,N_{\rm L}$, whereas for an asynchronous scenario, Δ_i's are modeled as deterministic unknown parameters. It is assumed that the signal component in (1) is contained completely in the observation interval $[T_{1,i}, T_{2,i}]$; that is, $\tau_i \in [T_{1,i}, T_{2,i} - T_{s,i}]$. In (1), the channel attenuation factor α_i is modeled as

$$\alpha_i = -\frac{(m_i+1)S}{2\pi} \frac{\left[(\boldsymbol{l}_{\rm r} - \boldsymbol{l}_{\rm t}^i)^T \boldsymbol{n}_{\rm t}^i\right]^{m_i} (\boldsymbol{l}_{\rm r} - \boldsymbol{l}_{\rm t}^i)^T \boldsymbol{n}_{\rm r}}{\|\boldsymbol{l}_{\rm r} - \boldsymbol{l}_{\rm t}^i\|^{m_i+3}} \tag{3}$$

where m_i is the Lambertian order for the ith LED transmitter, S is the area of the photo detector at the VLC receiver, and $\boldsymbol{n}_{\rm r} = [n_{{\rm r},1}\ n_{{\rm r},2}\ n_{{\rm r},3}]^T$ and $\boldsymbol{n}_{\rm t}^i = [n_{{\rm t},1}^i\ n_{{\rm t},2}^i\ n_{{\rm t},3}^i]^T$ denote the orientation vectors ('normals') of the VLC receiver and the ith LED transmitter, respectively [5], [23].[1] It is assumed that the VLC receiver knows S, $\boldsymbol{n}_{\rm r}$, m_i, $\boldsymbol{l}_{\rm t}^i$, and $\boldsymbol{n}_{\rm t}^i$ for $i = 1,\dots,N_{\rm L}$. For example, the orientation of the VLC receiver, $\boldsymbol{n}_{\rm r}$, can be determined by a gyroscope and the parameters of the LED transmitters (m_i, $\boldsymbol{l}_{\rm t}^i$ and $\boldsymbol{n}_{\rm t}^i$) can be sent to the receiver via visible light communications.

B. Log-Likelihood Function and CRLB

Considering the received signal model in (1), the log-likelihood function for the received signal vector $\boldsymbol{r}(t) \triangleq [r_1(t) \dots r_{N_{\rm L}}(t)]^T$ is obtained as follows [46], [47]:

$$\Lambda(\boldsymbol{\varphi}) = k - \frac{1}{2\sigma^2} \sum_{i=1}^{N_{\rm L}} \int_{T_{1,i}}^{T_{2,i}} \left(r_i(t) - \alpha_i R_p \, s_i(t-\tau_i)\right)^2 dt \tag{4}$$

where $\boldsymbol{\varphi}$ represents the set of unknown parameters and k is a normalizing constant that does not depend on the unknown parameters. While the set of unknown parameters consists only of the coordinates of the VLC receiver in the synchronous case, it also contains the delay parameters in the asynchronous case, as investigated in Sections III and IV.

The CRLB on the covariance matrix of any unbiased estimator $\hat{\boldsymbol{\varphi}}$ of $\boldsymbol{\varphi}$ can be expressed as [48]

$$\mathbb{E}\{(\hat{\boldsymbol{\varphi}} - \boldsymbol{\varphi})(\hat{\boldsymbol{\varphi}} - \boldsymbol{\varphi})^T\} \succeq \mathbf{J}(\boldsymbol{\varphi})^{-1} \tag{5}$$

where $\boldsymbol{A} \succeq \boldsymbol{B}$ means that $\boldsymbol{A} - \boldsymbol{B}$ is positive semidefinite and $\mathbf{J}(\boldsymbol{\varphi})$ is the Fisher information matrix (FIM) for $\boldsymbol{\varphi}$, which can be calculated as follows:

$$\mathbf{J}(\boldsymbol{\varphi}) = \mathbb{E}\left\{ \left(\nabla_{\boldsymbol{\varphi}} \Lambda(\boldsymbol{\varphi})\right) \left(\nabla_{\boldsymbol{\varphi}} \Lambda(\boldsymbol{\varphi})\right)^T \right\} \tag{6}$$

with $\nabla_{\boldsymbol{\varphi}}$ representing the gradient operator with respect to $\boldsymbol{\varphi}$ and $\Lambda(\boldsymbol{\varphi})$ being the log-likelihood function as defined in (4).

III. Positioning in Synchronous Systems

In the synchronous scenario, the VLC receiver is synchronized with the LED transmitters; that is, $\Delta_i = 0$ in (2) for $i = 1,\dots,N_{\rm L}$. In this section, the CRLB is derived for synchronous VLP systems, the direct position estimation is proposed, and the two-step position estimation is developed by considering both time delay and channel attenuation information.

A. CRLB

In the synchronous case, α_i and τ_i are functions of $\boldsymbol{l}_{\rm r}$ only (since $\Delta_i = 0$ in (2)); hence, the set of unknown parameters in (4) is defined as

$$\boldsymbol{\varphi} = [l_{{\rm r},1}\ l_{{\rm r},2}\ l_{{\rm r},3}]^T = \boldsymbol{l}_{\rm r}\,. \tag{7}$$

Then, the CRLB for estimating $\boldsymbol{l}_{\rm r}$ based on $r_1(t),\dots,r_{N_{\rm L}}(t)$ in (1) is specified by the following proposition.

[1] For example, if the VLC receiver is pointing up directly, then $\boldsymbol{n}_{\rm r} = [0\ 0\ 1]^T$.

Proposition 1*: For synchronous VLP systems, the CRLB on the mean-squared error (MSE) of any unbiased estimator $\hat{\boldsymbol{l}}_{\rm r}$ for the location of the VLC receiver is given by*

$$\mathbb{E}\{\|\hat{\boldsymbol{l}}_{\rm r}-\boldsymbol{l}_{\rm r}\|^2\}\geq \mathrm{trace}\{\mathbf{J}_{\rm syn}^{-1}\} \tag{8}$$

where

$$[\mathbf{J}_{\rm syn}]_{k_1,k_2}=\frac{R_p^2}{\sigma^2}\sum_{i=1}^{N_{\rm L}}\bigg(E_2^i\frac{\partial\alpha_i}{\partial l_{{\rm r},k_1}}\frac{\partial\alpha_i}{\partial l_{{\rm r},k_2}}+E_1^i\alpha_i^2\frac{\partial\tau_i}{\partial l_{{\rm r},k_1}}\frac{\partial\tau_i}{\partial l_{{\rm r},k_2}} - E_3^i\alpha_i\Big(\frac{\partial\alpha_i}{\partial l_{{\rm r},k_1}}\frac{\partial\tau_i}{\partial l_{{\rm r},k_2}}+\frac{\partial\tau_i}{\partial l_{{\rm r},k_1}}\frac{\partial\alpha_i}{\partial l_{{\rm r},k_2}}\Big)\bigg) \tag{9}$$

for $k_1,k_2\in\{1,2,3\}$ *with*

$$E_1^i\triangleq\int_0^{T_{s,i}}\big(s_i'(t)\big)^2dt \tag{10}$$

$$E_2^i\triangleq\int_0^{T_{s,i}}\big(s_i(t)\big)^2dt \tag{11}$$

$$E_3^i\triangleq\int_0^{T_{s,i}}s_i(t)s_i'(t)dt \tag{12}$$

$$\frac{\partial\tau_i}{\partial l_{{\rm r},k}}=\frac{l_{{\rm r},k}-l_{{\rm t},k}^i}{c\|\boldsymbol{l}_{\rm r}-\boldsymbol{l}_{\rm t}^i\|} \tag{13}$$

$$\frac{\partial\alpha_i}{\partial l_{{\rm r},k}}=-\frac{(m_i+1)S}{2\pi}\bigg(\frac{\big((\boldsymbol{l}_{\rm r}-\boldsymbol{l}_{\rm t}^i)^T\boldsymbol{n}_{\rm t}^i\big)^{m_i-1}}{\|\boldsymbol{l}_{\rm r}-\boldsymbol{l}_{\rm t}^i\|^{m_i+3}} \times\big(m_i\,n_{{\rm t},k}^i(\boldsymbol{l}_{\rm r}-\boldsymbol{l}_{\rm t}^i)^T\boldsymbol{n}_{\rm r}+n_{{\rm r},k}(\boldsymbol{l}_{\rm r}-\boldsymbol{l}_{\rm t}^i)^T\boldsymbol{n}_{\rm t}^i\big) - \frac{(m_i+3)(l_{{\rm r},k}-l_{{\rm t},k}^i)}{\|\boldsymbol{l}_{\rm r}-\boldsymbol{l}_{\rm t}^i\|^{m_i+5}}\big((\boldsymbol{l}_{\rm r}-\boldsymbol{l}_{\rm t}^i)^T\boldsymbol{n}_{\rm t}^i\big)^{m_i}(\boldsymbol{l}_{\rm r}-\boldsymbol{l}_{\rm t}^i)^T\boldsymbol{n}_{\rm r}\bigg). \tag{14}$$

Proof: Consider the likelihood function in (4), where τ_i and α_i are related to $\boldsymbol{l}_{\rm r}$ as in (2) (with $\Delta_i=0$) and (3), respectively. Since the set of unknown parameters in the synchronous case is equal to $\boldsymbol{l}_{\rm r}$ as stated in (7), the elements of the FIM in (6) can be expressed as

$$[\mathbf{J}(\boldsymbol{\varphi})]_{k_1,k_2}=\mathbb{E}\left\{\frac{\partial\Lambda(\boldsymbol{\varphi})}{\partial l_{{\rm r},k_1}}\frac{\partial\Lambda(\boldsymbol{\varphi})}{\partial l_{{\rm r},k_2}}\right\} \tag{15}$$

for $k_1,k_2\in\{1,2,3\}$. From (4), the expression in (15) can be calculated as follows:

$$[\mathbf{J}(\boldsymbol{\varphi})]_{k_1,k_2}=\frac{R_p^2}{\sigma^2}\sum_{i=1}^{N_{\rm L}}\bigg(E_2^i\frac{\partial\alpha_i}{\partial l_{{\rm r},k_1}}\frac{\partial\alpha_i}{\partial l_{{\rm r},k_2}} +\alpha_i\frac{\partial\alpha_i}{\partial l_{{\rm r},k_1}}\int_{T_{1,i}}^{T_{2,i}}s_i(t-\tau_i)\frac{\partial s_i(t-\tau_i)}{\partial l_{{\rm r},k_2}}dt +\alpha_i\frac{\partial\alpha_i}{\partial l_{{\rm r},k_2}}\int_{T_{1,i}}^{T_{2,i}}s_i(t-\tau_i)\frac{\partial s_i(t-\tau_i)}{\partial l_{{\rm r},k_1}}dt +\alpha_i^2\int_{T_{1,i}}^{T_{2,i}}\frac{\partial s_i(t-\tau_i)}{\partial l_{{\rm r},k_1}}\frac{\partial s_i(t-\tau_i)}{\partial l_{{\rm r},k_2}}dt\bigg) \tag{16}$$

where $E_2^i\triangleq\int_{T_{1,i}}^{T_{2,i}}s_i^2(t-\tau_i)dt$, which is equal to the expression in (11) as $s_i(t-\tau_i)$ is assumed to be contained completely in the observation interval $[T_{1,i},T_{2,i}]$. Since $\partial s_i(t-\tau_i)/\partial l_{{\rm r},k}=-(\partial\tau_i/\partial l_{{\rm r},k})s_i'(t-\tau_i)$, the expression in (16) can be shown to be equal to that in (9) based on the definitions in (10) and (12); hence, $\mathbf{J}(\boldsymbol{\varphi})=\mathbf{J}_{\rm syn}$. In addition, the partial derivatives in (13) and (14) can be obtained from (2) (with $\Delta_i=0$) and (3), respectively. Finally, the CRLB on the MSE of any unbiased estimator $\hat{\boldsymbol{l}}_{\rm r}$ for the location of the VLC receiver, $\boldsymbol{l}_{\rm r}$, can be expressed based on the inequality in (5) as

$$\mathrm{E}\{\|\hat{\boldsymbol{l}}_{\rm r}-\boldsymbol{l}_{\rm r}\|^2\}\geq\mathrm{trace}\{\mathbf{J}(\boldsymbol{\varphi})^{-1}\}. \tag{17}$$

Since $\mathbf{J}(\boldsymbol{\varphi})$ in (16) is equal to $\mathbf{J}_{\rm syn}$ in (9), as discussed above, the expression in (8) follows from (17). ■

The CRLB expression specified by (8)–(14) illustrates the effects of the transmitted signals via the E_1^i, E_2^i, and E_3^i parameters and the impact of the geometry (configuration) via the $\partial\tau_i/\partial l_{{\rm r},k}$ and $\partial\alpha_i/\partial l_{{\rm r},k}$ terms. Hence, the theoretical limit on the localization accuracy can be evaluated for any given system based on the provided expression. It is noted that the CRLB expression in Proposition 1 has not been available in the literature, and provides a theoretical limit for synchronous VLP systems by utilizing information from both channel attenuation factors (RSS) and time delay parameters (TOA). Compared to the CRLB in Proposition 1, those in [5], [6], [25] are for distance estimation only, and those in [23], [37], [38] focus on RSS based localization. As noted from Proposition 1 and its proof, the main technical difference and difficulty in obtaining the proposed CRLB expression is related to the simultaneous use of the TOA and RSS parameters, which requires the calculation of the partial derivatives of both $\{\alpha_i\}_{i=1}^{N_{\rm L}}$ and $\{\tau_i\}_{i=1}^{N_{\rm L}}$.

The CRLB expression in Proposition 1 is generic since the LED transmitters and the VLC receiver can have any locations and orientations and the transmitted signals can be in generic forms. Special cases can easily be obtained from (8)–(14). For example, if the transmitted signals satisfy $s_i(T_{s,i})=s_i(0)$ for $i=1,\ldots,N_{\rm L}$, then E_3^i in (12) becomes zero[2] and $[\mathbf{J}_{\rm syn}]_{k_1,k_2}$ in (9) reduces to

$$[\mathbf{J}_{\rm syn}]_{k_1,k_2}=\frac{R_p^2}{\sigma^2}\sum_{i=1}^{N_{\rm L}}\bigg(E_2^i\frac{\partial\alpha_i}{\partial l_{{\rm r},k_1}}\frac{\partial\alpha_i}{\partial l_{{\rm r},k_2}}+E_1^i\alpha_i^2\frac{\partial\tau_i}{\partial l_{{\rm r},k_1}}\frac{\partial\tau_i}{\partial l_{{\rm r},k_2}}\bigg) \tag{18}$$

From (18), the contribution of the channel attenuation factors and time delays can be observed individually. Namely, the first and the second elements in (18) are related to the location information obtained from the channel attenuation factors and the time delay parameters, respectively. Hence, it is noted that both RSS and TOA parameters are utilized for localization in the synchronous scenario.

B. Direct Positioning

Direct positioning refers to the estimation of the unknown location directly from the received signals without any intermediate steps for estimating location related parameters such as TOA or RSS [26]–[28], [30]–[33], [35], [36] (cf. Section III-C). Direct positioning has not been considered before for synchronous VLP systems, which carry significant differences from RF based positioning systems.

In direct positioning, the aim is to estimate the location of the VLC receiver, $\boldsymbol{l}_{\rm r}$, based on the received signals in (1).

[2]Since $E_3^i=\int_0^{T_{s,i}}s_i(t)s_i'(t)dt=(s_i(T_{s,i})^2-s_i(0)^2)/2$, $E_3^i=0$ if $s_i(T_{s,i})=s_i(0)$, which is satisfied for most practical pulse shapes (cf. (52) and [5, Eq. 3]).

From (4) and (7), the ML estimator for $\boldsymbol{l}_{\rm r}$ can be obtained as follows [48]:

$$\hat{\boldsymbol{l}}_{\rm r}^{\rm DP,syn} = \arg\max_{\boldsymbol{l}_{\rm r}} \; -\sum_{i=1}^{N_{\rm L}} \int_{T_{1,i}}^{T_{2,i}} \left(r_i(t) - \alpha_i R_p \, s_i(t-\tau_i)\right)^2 dt$$

which can be simplified, after some manipulation, into

$$\hat{\boldsymbol{l}}_{\rm r}^{\rm DP,syn} = \arg\max_{\boldsymbol{l}_{\rm r}} \; \sum_{i=1}^{N_{\rm L}} \alpha_i \int_{T_{1,i}}^{T_{2,i}} r_i(t) s_i(t-\tau_i) dt - \frac{R_p}{2} \sum_{i=1}^{N_{\rm L}} \alpha_i^2 E_2^i \tag{19}$$

where E_2^i is as defined in (11). It should be noted that τ_i and α_i in (19) are functions of $\boldsymbol{l}_{\rm r}$ as specified in (2) (with $\Delta_i = 0$) and (3), respectively. Hence, the direct ML position estimator in (19) searches over all possible values of the unknown position $\boldsymbol{l}_{\rm r}$ based on the relations of $\boldsymbol{l}_{\rm r}$ with the channel attenuation factors and the time delays.

The main advantage of the direct positioning approach in (19) is related to its performance (optimality in the ML sense), as investigated in Section V. On the other hand, it can lead to high complexity in certain applications due to increased storage and communication requirements. For example, if the location estimation should be performed at a central unit, then it becomes cumbersome to transmit all the received signals to the center.

C. Two-Step Positioning

A common method for positioning in wireless networks is to apply a two-step estimation process where estimation of location related parameters such as RSS, TOA, TDOA, and/or AOA is performed in the first step and the unknown location is estimated based on those parameters in the second step [19].

Although two-step positioning has commonly been considered for VLP systems (e.g., [9], [15], [17], [18], [22]–[24], [43]), there exist no studies on the design of two-step estimators for synchronous VLP systems in which both RSS and TOA information can be utilized. In the proposed two-step estimator for synchronous VLP systems, the ML estimates of the TOA and RSS parameters are obtained for each of the $N_{\rm L}$ LED transmitters in the first step, and the location of the VLC receiver is estimated based on those location related parameters, i.e., TOA and RSS estimates, in the second step.

In the first step, the ML estimates of the TOA and RSS parameters[3] are obtained for each LED transmitter. For the ith LED transmitter, the received signal $r_i(t)$ is expressed as in (1) and the corresponding log-likelihood function for $r_i(t)$ is given by $k_i - \frac{1}{2\sigma^2}\int_{T_{1,i}}^{T_{2,i}} \left(r_i(t) - \alpha_i R_p \, s_i(t-\tau_i)\right)^2 dt$, where k_i is a constant that does not depend on α_i and τ_i (cf. (4)). Then, the ML estimates of the TOA and RSS parameters corresponding to the ith LED transmitter are obtained as follows:

$$(\hat{\tau}_i, \hat{\alpha}_i) = \arg\max_{(\tau_i,\alpha_i)} \; 2\alpha_i \int_{T_{1,i}}^{T_{2,i}} r_i(t) s_i(t-\tau_i) dt - \alpha_i^2 R_p E_2^i \tag{20}$$

[3]The channel attenuation factor α_i is referred to as the RSS parameter in this study since $\alpha_i \geq 0$ in visible light channels and it determines the received signal energy (power).

for $i = 1, \ldots, N_{\rm L}$. Since α_i is nonnegative, the solution for $\hat{\tau}_i$ is obtained by maximizing the integral expression in (20). Hence, the ML estimate $\hat{\tau}_i$ of the TOA parameter τ_i for the ith LED transmitter is calculated from

$$\hat{\tau}_i = \arg\max_{\tau_i} \int_{T_{1,i}}^{T_{2,i}} r_i(t) s_i(t-\tau_i) dt \, . \tag{21}$$

Then, $\hat{\alpha}_i$ can be expressed from (20) and (21) as

$$\hat{\alpha}_i = \arg\max_{\alpha_i} \; 2\alpha_i \tilde{C}_{rs}^i - \alpha_i^2 R_p E_2^i \tag{22}$$

where

$$\tilde{C}_{rs}^i \triangleq \int_{T_{1,i}}^{T_{2,i}} r_i(t) s_i(t-\hat{\tau}_i) dt \, . \tag{23}$$

The problem in (22) leads to the following closed-form expression for the ML estimate of the RSS parameter α_i corresponding to the ith LED transmitter:

$$\hat{\alpha}_i = \frac{\tilde{C}_{rs}^i}{R_p E_2^i} \, . \tag{24}$$

In the second step, the aim is to estimate the location of the VLC receiver, $\boldsymbol{l}_{\rm r}$, based on the TOA and RSS estimates in the first step; that is, $\{\hat{\alpha}_i, \hat{\tau}_i\}_{i=1}^{N_{\rm L}}$. To that aim, the following lemma is presented first in order to characterize the statistics of the estimates obtained in the first step.

Lemma 1*: Assume that $E_3^i = 0$ for $i = 1, \ldots, N_{\rm L}$. Then, at high SNRs (i.e., for $\alpha_i^2 R_p^2 E_2^i \gg \sigma^2$), the TOA estimate in* (21) *and the RSS estimate in* (24) *can approximately be modeled as*

$$\hat{\tau}_i = \tau_i + \nu_i \tag{25}$$

$$\hat{\alpha}_i = \alpha_i + \varsigma_i \tag{26}$$

for $i = 1, \ldots, N_{\rm L}$, where ν_i and ς_i are independent zero mean Gaussian random variables with variances $\sigma^2/(R_p^2 \alpha_i^2 E_1^i)$ and $\sigma^2/(R_p^2 E_2^i)$, respectively, and ν_i and ν_j (ς_i and ς_j) are independent for $i \neq j$.

Proof: Please see Appendix A.

Lemma 1 states the asymptotic unbiasedness and efficiency properties of the ML estimates $\hat{\tau}_i$ in (21) and $\hat{\alpha}_i$ in (24) [48], [49]. Based on Lemma 1, the following estimator can be obtained for the second step of the two-step estimator:

$$\hat{\boldsymbol{l}}_{\rm r}^{\rm TS,syn} = \arg\min_{\boldsymbol{l}_{\rm r}} \sum_{i=1}^{N_{\rm L}} \left(E_1^i \alpha_i^2 \left(\hat{\tau}_i - \tau_i\right)^2 + E_2^i \left(\hat{\alpha}_i - \alpha_i\right)^2 \right) - \frac{2\sigma^2}{R_p^2} \sum_{i=1}^{N_{\rm L}} \log \alpha_i \tag{27}$$

where τ_i and α_i are functions of $\boldsymbol{l}_{\rm r}$ as defined in (2) (with $\Delta_i = 0$) and (3), respectively, and $\log$ denotes the natural logarithm. The estimator in (27) corresponds to the ML estimator for $\boldsymbol{l}_{\rm r}$ based on the TOA and RSS estimates in the first step when they are Gaussian distributed as specified in Lemma 1 (please see Appendix B for the derivation). In other words, at high SNRs, $\hat{\boldsymbol{l}}_{\rm r}^{\rm TS,syn}$ in (27) is approximately the ML estimator for $\boldsymbol{l}_{\rm r}$ based on $\{\hat{\alpha}_i, \hat{\tau}_i\}_{i=1}^{N_{\rm L}}$. Since the last term in (27) is commonly

smaller than the others at high SNRs, a simpler version of (27) can be proposed as follows:

$$\hat{\boldsymbol{l}}_{\mathrm{r}}^{\mathrm{TS,syn}} = \arg\min_{\boldsymbol{l}_{\mathrm{r}}} \sum_{i=1}^{N_{\mathrm{L}}} \left(E_1^i \hat{\alpha}_i{}^2 \left(\hat{\tau}_i - \tau_i\right)^2 + E_2^i \left(\hat{\alpha}_i - \alpha_i\right)^2 \right) \tag{28}$$

where the estimate $\hat{\alpha}_i$ is replaced with α_i in the first term, as well, considering high SNRs. The simplified estimator in (28) corresponds to a nonlinear least-squares (NLS) estimator.

In summary, the proposed two-step positioning approach first calculates the TOA and RSS estimates via (21) and (24) for each LED transmitter, and then uses those estimates for determining the position of the VLC receiver via (28). In Section V, comparisons between the two-step and direct positioning approaches are provided via simulations. In order to present a theoretical comparison under the conditions in Lemma 1, the following proposition specifies the CRLB for estimating the VLC receiver location, $\boldsymbol{l}_{\mathrm{r}}$, based on the TOA and RSS estimates $\{\hat{\alpha}_i, \hat{\tau}_i\}_{i=1}^{N_{\mathrm{L}}}$ obtained in the first step.

Proposition 2*: Suppose that the conditions in Lemma 1 hold. Then, the CRLB on the MSE of any unbiased estimator $\hat{\boldsymbol{l}}_{\mathrm{r}}$ for the location of the VLC receiver, $\boldsymbol{l}_{\mathrm{r}}$, based on the TOA and RSS estimates $\{\hat{\alpha}_i, \hat{\tau}_i\}_{i=1}^{N_{\mathrm{L}}}$ obtained from* (21) *and* (24)*, is stated as*

$$\mathbb{E}\{\|\hat{\boldsymbol{l}}_{\mathrm{r}} - \boldsymbol{l}_{\mathrm{r}}\|^2\} \geq \mathrm{trace}\{\mathbf{J}_{\mathrm{TS,syn}}^{-1}\} \tag{29}$$

where $\mathbf{J}_{\mathrm{TS,syn}}$ is a 3×3 matrix with the following elements:

$$[\mathbf{J}_{\mathrm{TS,syn}}]_{k_1,k_2} = \frac{R_p^2}{\sigma^2} \sum_{i=1}^{N_{\mathrm{L}}} \left(E_2^i \frac{\partial \alpha_i}{\partial l_{\mathrm{r},k_1}} \frac{\partial \alpha_i}{\partial l_{\mathrm{r},k_2}} + E_1^i \alpha_i^2 \frac{\partial \tau_i}{\partial l_{\mathrm{r},k_1}} \frac{\partial \tau_i}{\partial l_{\mathrm{r},k_2}} \right) \tag{30}$$

for $k_1, k_2 \in \{1,2,3\}$, with E_1^i, E_2^i, $\partial\tau_i/\partial l_{\mathrm{r},k}$ and $\partial\alpha_i/\partial l_{\mathrm{r},k}$ being as defined in (10)*,* (11)*,* (13) *and* (14)*, respectively.*

Proof: Please see Appendix C.

The CRLB expression in Proposition 2 presents an important guideline for asymptotic comparison of the direct and two-step positioning approaches in synchronous VLP systems as detailed in the following remark.

Remark 1: It is observed that the expression in (18), which is obtained for direct positioning under the assumption of $E_3^i = 0$, is equal to that in (30), which is for two-step positioning under the assumptions of $E_3^i = 0$ and $\alpha_i^2 R_p^2 E_2^i \gg \sigma^2$. In other words, referring to the signal model in (1), the performance of direct positioning and two-step positioning algorithms converges to each other at high SNRs. Hence, it can be concluded that the benefits of direct positioning are more prominent in the low SNR regime, which is in compliance with the results obtained for RF systems [26], [31]. This conclusion is intuitive since the consistency between TOA and RSS estimates (measurements) gets higher as the SNR increases. In the low SNR regime, the TOA estimate in (21) may be far away from the true time delay, leading possibly to a mismatch between the corresponding RSS estimate in (24) and the position information inferred from that TOA information. In such cases, the direct positioning approach is capable of estimating the unknown location more accurately than the two-step approach by utilizing entire signals and thus producing consistent location estimates.

D. Complexity Analysis

In this part, computational complexity analyses are presented for the proposed direct and two-step estimators in Section III-B and Section III-C.

Consider an indoor localization scenario where the VLC receiver moves inside a certain volume and tries to estimate its position. Then, complexity analyses can be performed by implementing the direct ML estimator in (19) and the two-step ML estimator in (28) over a finite search space corresponding to that volume for the location of the VLC receiver. Since the objective functions in (19) and (28) are nonconvex with respect to the VLC receiver location, $\boldsymbol{l}_{\mathrm{r}}$, the exhaustive search method is considered for identifying the global optimum. For complexity calculations, it is assumed that range (or, equivalently, time) dimensions are sampled with a sampling interval on the order of Δd. To that aim, we consider a three-dimensional uniform grid $\mathcal{U}$ consisting of $\mathcal{O}(1/\Delta d^3)$ possible locations in the considered volume for the location of the VLC receiver. Based on $\mathcal{U}$, the complexity analyses for the direct and two-step positioning algorithms are provided as follows.

1) Direct Positioning: For the computation of the objective function in (19) at each search location $\boldsymbol{l}_{\mathrm{r}} \in \mathcal{U}$, it is necessary to compute α_i via (3), τ_i via (2), and the correlator output $\int_{T_{1,i}}^{T_{2,i}} r_i(t) s_i(t-\tau_i) dt$ using the computed τ_i value. First, the computation of α_i in (3) and τ_i in (2) has $\mathcal{O}(1)$ complexity since these operations take a constant time for a given value of $\boldsymbol{l}_{\mathrm{r}}$. Secondly, evaluating the integral $\int_{T_{1,i}}^{T_{2,i}} r_i(t) s_i(t-\tau_i) dt$ requires $\mathcal{O}(1/\Delta d)$ operations. Taking into account the whole search space $\mathcal{U}$ (which contains $\mathcal{O}(1/\Delta d^3)$ points) and all N_{L} LEDs, the overall complexity of the direct positioning method becomes

$$\mathcal{O}(N_{\mathrm{L}} \times 1/\Delta d^4) \ . \tag{31}$$

2) Two-Step Positioning: In the first step of the two-step estimator in (28), $\hat{\tau}_i$ in (21) and $\hat{\alpha}_i$ in (24) must be computed. Assuming that continuous signals are sampled with the number of samples on the order of $\mathcal{O}(1/\Delta d)$, as in direct positioning, the computation of the integral expression in (21) requires $\mathcal{O}(1/\Delta d)$ operations for a given τ_i. Since τ_i lies in the finite interval $[T_{1,i}, T_{2,i} - T_{s,i}]$, it can be assumed that there exists $\mathcal{O}(1/\Delta d)$ different values of τ_i. Hence, the overall complexity of (21) becomes $\mathcal{O}(1/\Delta d^2)$. On the other hand, the computation of $\hat{\alpha}_i$ via (24) has a computational complexity of $\mathcal{O}(1)$ once the results of (21) and (23) are obtained. In the second step, τ_i and α_i in (28) must be evaluated for each $\boldsymbol{l}_{\mathrm{r}} \in \mathcal{U}$, whose size is on the order of $\mathcal{O}(1/\Delta d^3)$. Therefore, the computational complexity of the two-step positioning is given by

$$\underbrace{\mathcal{O}(N_{\mathrm{L}} \times 1/\Delta d^2)}_{\text{First Step}} + \underbrace{\mathcal{O}(N_{\mathrm{L}} \times 1/\Delta d^3)}_{\text{Second Step}} = \mathcal{O}(N_{\mathrm{L}} \times 1/\Delta d^3) \tag{32}$$

where the term corresponding to the second step calculations dominates as the sampling interval Δd approaches zero.

The proposed direct and two-step positioning approaches can be compared based on the expressions in (31) and (32) in terms of the computational complexity. For instance, if Δd is sufficiently small, i.e., range/time dimensions are sampled fast enough to achieve high resolution, then the direct position estimator has a higher complexity than its two-step counterpart. Moreover, it is observed, by comparing (31) and (32), that the task of integral evaluation is performed at each search location $\boldsymbol{l}_{\rm r} \in \mathcal{U}$ in direct positioning, whereas it only appears in the first-step calculations in two-step positioning. This alleviates the strain on the second-step calculations in the two-step approach, which makes it computationally less demanding than the direct approach. Hence, the main computational burden of direct positioning consists in evaluating the correlator output $\int_{T_{1,i}}^{T_{2,i}} r_i(t)s_i(t-\tau_i)dt$ at each search location $\boldsymbol{l}_{\rm r}$.

IV. Positioning in Asynchronous Systems

In the asynchronous scenario, the VLC receiver is not synchronized with the LED transmitters; that is, Δ_i in (2) is a deterministic unknown parameter for each $i \in \{1,\dots,N_{\rm L}\}$. In this section, the CRLB is derived for asynchronous VLP systems, and the direct position estimation and its relation to the two-step position estimation are investigated.

A. CRLB

In an asynchronous VLP system, the unknown parameters include the TOAs of the received signals coming from the LED transmitters in addition to the location of the VLC receiver. Hence, the vector of unknown parameters in (4) for the asynchronous case can be expressed as

$$\boldsymbol{\varphi} = \left[l_{{\rm r},1}\ l_{{\rm r},2}\ l_{{\rm r},3}\ \tau_1\ \dots\ \tau_{N_{\rm L}}\right]^T. \tag{33}$$

Then, the CRLB for estimating $\boldsymbol{l}_{\rm r}$ based on $r_1(t),\dots,r_{N_{\rm L}}(t)$ in (1) is stated in the following proposition.

Proposition 3*: For asynchronous VLP systems, the CRLB on the MSE of any unbiased estimator $\hat{\boldsymbol{l}}_{\rm r}$ for the location of the VLC receiver is given by*

$$\mathbb{E}\{\|\hat{\boldsymbol{l}}_{\rm r} - \boldsymbol{l}_{\rm r}\|^2\} \geq {\rm trace}\{\mathbf{J}_{\rm asy}^{-1}\} \tag{34}$$

where $\mathbf{J}_{\rm asy}$ denotes a 3×3 matrix with the following elements:

$$[\mathbf{J}_{\rm asy}]_{k_1,k_2} = \frac{R_p^2}{\sigma^2}\sum_{i=1}^{N_{\rm L}}\left(E_2^i - \frac{(E_3^i)^2}{E_1^i}\right)\frac{\partial\alpha_i}{\partial l_{{\rm r},k_1}}\frac{\partial\alpha_i}{\partial l_{{\rm r},k_2}} \tag{35}$$

for $k_1,k_2 \in \{1,2,3\}$, with E_1^i, E_2^i, E_3^i, and $\partial\alpha_i/\partial l_{{\rm r},k}$ being as defined in (10), (11), (12), *and* (14), *respectively.*

Proof: Consider the log-likelihood function in (4) for the unknown parameter vector in (33). Then, from (6), the FIM can be obtained after some manipulation as

$$\mathbf{J}(\boldsymbol{\varphi}) = \begin{bmatrix}\mathbf{J_A} & \mathbf{J_B}\\ \mathbf{J_B}^T & \mathbf{J_D}\end{bmatrix} \tag{36}$$

where $\mathbf{J_A}$ is a 3×3 matrix with elements

$$[\mathbf{J_A}]_{k_1,k_2} = \frac{R_p^2}{\sigma^2}\sum_{i=1}^{N_{\rm L}} E_2^i\frac{\partial\alpha_i}{\partial l_{{\rm r},k_1}}\frac{\partial\alpha_i}{\partial l_{{\rm r},k_2}} \tag{37}$$

for $k_1,k_2 \in \{1,2,3\}$, $\mathbf{J_B}$ is a $3\times N_{\rm L}$ matrix with elements

$$[\mathbf{J_B}]_{k,i} = -\frac{R_p^2}{\sigma^2}E_3^i\alpha_i\frac{\partial\alpha_i}{\partial l_{{\rm r},k}} \tag{38}$$

for $k\in\{1,2,3\}$ and $i\in\{1,\dots,N_{\rm L}\}$, and $\mathbf{J_D}$ is an $N_{\rm L}\times N_{\rm L}$ matrix with elements

$$[\mathbf{J_D}]_{i_1,i_2} = \begin{cases}\frac{R_p^2}{\sigma^2}\alpha_{i_1}^2 E_1^{i_1}, & \text{if } i_1 = i_2\\ 0, & \text{if } i_1 \neq i_2\end{cases} \tag{39}$$

for $i_1,i_2 \in \{1,\dots,N_{\rm L}\}$. In (37)–(39), E_1^i, E_2^i, E_3^i, and $\partial\alpha_i/\partial l_{{\rm r},k}$ are as defined in (10), (11), (12), and (14), respectively.

The CRLB on the location $\boldsymbol{l}_{\rm r}$ of the VLC receiver can be expressed, based on (5), as

$$\mathbb{E}\{\|\hat{\boldsymbol{l}}_{\rm r} - \boldsymbol{l}_{\rm r}\|^2\} \geq {\rm trace}\Big\{\left[\mathbf{J}^{-1}(\boldsymbol{\varphi})\right]_{3\times 3}\Big\} \tag{40}$$

where $\hat{\boldsymbol{l}}_{\rm r}$ is any unbiased estimator for $\boldsymbol{l}_{\rm r}$. From (36), $\left[\mathbf{J}^{-1}(\boldsymbol{\varphi})\right]_{3\times 3}$ can be stated as

$$\left[\mathbf{J}^{-1}(\boldsymbol{\varphi})\right]_{3\times 3} = \left(\mathbf{J_A} - \mathbf{J_B}\mathbf{J_D}^{-1}\mathbf{J_B}\right)^{-1}. \tag{41}$$

Based on (37)–(39), $\mathbf{J_A} - \mathbf{J_B}\mathbf{J_D}^{-1}\mathbf{J_B}$ can be calculated after some manipulation as

$$\left[\mathbf{J_A} - \mathbf{J_B}\mathbf{J_D}^{-1}\mathbf{J_B}\right]_{k_1,k_2} = \frac{R_p^2}{\sigma^2}\sum_{i=1}^{N_{\rm L}}\left(E_2^i - \frac{(E_3^i)^2}{E_1^i}\right)\frac{\partial\alpha_i}{\partial l_{{\rm r},k_1}}\frac{\partial\alpha_i}{\partial l_{{\rm r},k_2}}. \tag{42}$$

Hence, (40)–(42) lead to the expressions in (34) and (35) in the proposition. ■

It is noted from the CRLB expression in Proposition 3 that the position related information in the channel attenuation factors (RSS) is utilized in the asynchronous case for estimating the location of the VLC receiver (see (35)). On the other hand, information from both the channel attenuation factors (RSS) and the time delay (TOA) parameters is available in the synchronous case as can be noted from Proposition 1. In addition, the CRLB expression presented in Proposition 3 has been obtained for the first time in the literature; hence, provides a theoretical contribution to localization in asynchronous VLP systems. Since the expression in (35) is obtained based on the entire observation signals, $r_i(t)$'s in (1), it differs from the CRLB expression in [23], which is derived for asynchronous VLP systems based on the RSS measurements without directly using the received signals (eqn. (32) in [23]). On the other hand, when $E_3^i = 0$ for $i = 1,\dots,N_{\rm L}$, which is valid for many practical pulses, the FIM expression in (35) is equivalent to that in [23]. Hence, the CRLB provided by Proposition 3 also covers the more general case of $E_3^i \neq 0$ as compared to the CRLB in [23], which constitutes a special case of (35).[4]

Remark 2: From Proposition 1 and Proposition 3, it is observed that if $E_3^i = 0$ and $\alpha_i^2 E_1^i \ll E_2^i$ for $i = 1,\dots,N_{\rm L}$, the CRLB expressions in the synchronous and asynchronous

[4]Indeed, it is proved in Proposition 4 in Section IV-B that the direct positioning approach adopted for the derivation of (35) is equivalent to the two-step method for asynchronous VLP systems under the condition of $E_3^i = 0$. This result explains the equivalence of the two expressions in (35) and [23] for practical localization scenarios.

cases converge to each other. This corresponds to scenarios in which the position related information in the time delay (TOA) parameters is negligible compared to that in the channel attenuation factors (RSS parameters). Hence, synchronism does not provide any significant benefits in such scenarios. Since E_1^i/E_2^i can be expressed from Parseval's relation as $4\pi^2\beta_i^2$, where β_i is the effective bandwidth of $s_i(t)$,[5] it can be concluded that the synchronous and asynchronous cases lead to similar CRLBs when the transmitted signals have small effective bandwidths. This is an intuitive result because TOA information gets less accurate as the effective bandwidth decreases [19].

B. Direct and Two-Step Estimation

Direct position estimation involves the estimation of $\boldsymbol{l}_{\rm r}$, the location of the VLC receiver, directly from the received signals in (1). From (4), the ML estimator for direct positioning in the asynchronous case can be obtained as follows:

$$\hat{\boldsymbol{\varphi}}_{\rm ML} = \arg\max_{\boldsymbol{\varphi}} \sum_{i=1}^{N_{\rm L}} \left(\alpha_i \int_{T_{1,i}}^{T_{2,i}} r_i(t) s_i(t-\tau_i) dt - \frac{R_p}{2} \alpha_i^2 E_2^i \right) \tag{43}$$

where $\boldsymbol{\varphi}$ is defined by (33), α_i is related to $\boldsymbol{l}_{\rm r}$ as in (3), and E_2^i is given by (11). Since α_i's are nonnegative and the integral expressions depend only on τ_i's (43), the ML estimates for τ_i's can be calculated as in (21). Then, the ML estimate for $\boldsymbol{l}_{\rm r}$ is obtained from (43) as

$$\hat{\boldsymbol{l}}_{\rm r}^{\rm DP,asy} = \arg\max_{\boldsymbol{l}_{\rm r}} \sum_{i=1}^{N_{\rm L}} \left(\alpha_i \tilde{C}_{rs}^i - 0.5 R_p \alpha_i^2 E_2^i \right) \tag{44}$$

where $\tilde{C}_{rs}^i$ is as defined in (23).

For the two-step position estimation in the asynchronous case, the RSS parameters related to $N_{\rm L}$ LED transmitters are estimated in the first step and the location of the VLC receiver is estimated based on those RSS estimates in the second step. Due to the asynchronism between the LED transmitters and the VLC receiver, the TOA parameters cannot be related to the location of the VLC receiver (see (2)); hence, cannot be utilized for positioning in this case (cf. Section III-C).

In the first step of the two-step estimator, the ML estimator for the RSS parameter, α_i, is calculated based on $r_i(t)$ for $i = 1, \ldots, N_{\rm L}$. Similar to that in the synchronous case (see Section III-C), the ML estimate $\hat{\alpha_i}$ of α_i is expressed as

$$\hat{\alpha_i} = \frac{\tilde{C}_{rs}^i}{R_p E_2^i} \tag{45}$$

for $i = 1, \ldots, N_{\rm L}$, where $\tilde{C}_{rs}^i$ is as in (23) and E_2^i is given by (11).

The second step utilizes the RSS estimates in (45) for $i = 1, \ldots, N_{\rm L}$ for estimating the location of the VLC receiver based on the following NLS estimator:

$$\hat{\boldsymbol{l}}_{\rm r}^{\rm TS,asy} = \arg\min_{\boldsymbol{l}_{\rm r}} \sum_{i=1}^{N_{\rm L}} w_i (\hat{\alpha_i} - \alpha_i)^2 \tag{46}$$

[5]The effective bandwidth is defined as $\beta_i = \sqrt{(1/E_2^i) \int f^2 |S_i(f)|^2 df}$, where $S_i(f)$ is the Fourier transform of $s_i(t)$.

where α_i is as defined in (3) and the following expression is proposed for the weighing coefficients:

$$w_i = \frac{\left(E_1^i E_2^i - (E_3^i)^2\right)}{E_1^i} \tag{47}$$

for $i = 1, \ldots, N_{\rm L}$, where E_1^i and E_3^i are as in (10) and (12), respectively. As illustrated in Appendix D, the proposed weighting coefficient in (47) is inversely proportional to the CRLB for estimating α_i from $r_i(t)$. Hence, the RSS estimates with higher accuracy (i.e., lower CRLBs) are assigned higher weights in the NLS estimator in (46).

In the following proposition, it is shown that the direct position estimator in (44) is equivalent to the two-step estimator specified by (45)–(47) under certain conditions.

Proposition 4: *Consider an asynchronous VLP system with $E_3^i = 0$ for $i = 1, \ldots, N_{\rm L}$. Then, the direct position estimator in* (44) *is equivalent to the two-step position estimator in* (45)–(47).

Proof: When $E_3^i = 0$, the weighting coefficient in (47) reduces to

$$w_i = E_2^i \tag{48}$$

for $i = 1, \ldots, N_{\rm L}$. Inserting (45) and (48) into (46) yields the following:

$$\hat{\boldsymbol{l}}_{\rm r}^{\rm TS,asy} = \arg\min_{\boldsymbol{l}_{\rm r}} \sum_{i=1}^{N_{\rm L}} E_2^i \left(\frac{\tilde{C}_{rs}^i}{R_p E_2^i} - \alpha_i \right)^2. \tag{49}$$

After some manipulation, the estimator in (49) can be expressed as

$$\hat{\boldsymbol{l}}_{\rm r}^{\rm TS,asy} = \arg\min_{\boldsymbol{l}_{\rm r}} \sum_{i=1}^{N_{\rm L}} \left(-2\alpha_i \tilde{C}_{rs}^i + \alpha_i^2 R_p E_2^i \right) \tag{50}$$

which is equivalent to the direct position estimator in (44). ■

Proposition 4 implies that the two-step position estimator is optimal in the ML sense for asynchronous VLP systems; that is, the direct positioning (based on ML estimation) is equivalent to the two-step positioning when $E_3^i = 0$ for $i = 1, \ldots, N_{\rm L}$. Since $s_i(0) = s_i(T_{s,i})$ for many practical pulses, $E_3^i = 0$ is encountered in practice (see (12)); hence, the two-step estimator can be employed in real systems as the optimal approach in the ML sense.

Remark 3: As proved in Proposition 4, if $E_3^i = 0$ for $i = 1, \ldots, N_{\rm L}$, the direct positioning approach is equivalent to the two-step approach for the asynchronous scenario, whereas Remark 1 states that the two approaches are only *asymptotically* equivalent for the synchronous scenario. The intuition behind these results is that the measurement of RSS information is performed at the peak of the correlator output over the observation interval, irrespective of the true time delay of the received signal. Hence, direct positioning reduces to two-step positioning for the asynchronous case. On the other hand, when the TOA information corresponding to the location of the correlator peak is incorporated into the estimation process in the synchronous case, the direct positioning approach can identify a more accurate location that accounts for the observed signal, which is also implied in Remark 1.

C. Complexity Analysis

In this part, the complexity analysis is performed for the proposed ML position estimators in Section IV-B. Specifically, the computational complexity of the direct estimator in (44) is investigated as in Section III-D.[6] First, $\tilde{C}^i_{rs}$ can be computed via (23) and (21) using $\mathcal{O}(1/\Delta d^2)$ operations. Then, for each $\boldsymbol{l}_{\rm r} \in \mathcal{U}$ and $i \in \{1, \ldots, N_{\rm L}\}$, the summand in (44) requires $\mathcal{O}(1)$ operations. Therefore, the overall complexity of the ML estimator in asynchronous VLP systems is obtained as

$$\mathcal{O}(N_{\rm L} \times 1/\Delta d^2) + \mathcal{O}(N_{\rm L} \times 1/\Delta d^3) = \mathcal{O}(N_{\rm L} \times 1/\Delta d^3) \ . \tag{51}$$

It follows from (31), (32) and (51) that the asynchronous estimator has the same order of complexity as that of the synchronous TS estimator and a lower complexity than the synchronous DP estimator.

V. Numerical Results

In this section, numerical results are presented to corroborate the theoretical derivations in the previous sections. As in [5], the responsivity of the photo detector is taken as $R_p = 0.4\,$mA/mW, and the spectral density level of the noise is set to $\sigma^2 = 1.336 \times 10^{-22}\,$W/Hz. In addition, the Lambertian order is taken as $m = 1$ and the area S of the photo detector at the VLC receiver is equal to $1\,\text{cm}^2$. The transmitted signal $s(t)$ in (1) is modeled as [5]

$$s(t) = A\left(1 - \cos\left(2\pi\, t/T_s\right)\right)\left(1 + \cos(2\pi f_c t)\right)\mathbb{I}_{t\in[0,T_s]} \tag{52}$$

where f_c denotes the center frequency, A corresponds to the average emitted optical power; that is, source optical power, and $\mathbb{I}_{t\in[0,T_s]}$ represents an indicator function, which is equal to 1 if $t \in [0, T_s]$ and zero otherwise.

We consider a room with a width, depth, and height of $[8\ 8\ 5]$ m, respectively, where $N_{\rm L} = 4$ LED transmitters are attached to the ceiling at positions $\boldsymbol{l}^1_{\rm t} = [2\ 2\ 5]^T$ m, $\boldsymbol{l}^2_{\rm t} = [6\ 2\ 5]^T$ m, $\boldsymbol{l}^3_{\rm t} = [2\ 6\ 5]^T$ m, and $\boldsymbol{l}^4_{\rm t} = [6\ 6\ 5]^T$ m, as illustrated in Fig. 1. The orientation vectors of the LEDs are given by

$$\boldsymbol{n}^i_{\rm t} = [\sin\theta_i \cos\phi_i \ \ \sin\theta_i \sin\phi_i \ \ \cos\theta_i]^T \tag{53}$$

for $i = 1, \ldots, N_{\rm L}$, where θ_i and ϕ_i denote the polar and the azimuth angles, respectively [50].[7] In the configuration in Fig. 1, the polar and the azimuth angles are taken as $(\theta_1, \phi_1) = (150°, 45°)$, $(\theta_2, \phi_2) = (150°, 135°)$, $(\theta_3, \phi_3) = (150°, -45°)$ and $(\theta_4, \phi_4) = (150°, -135°)$. The VLC receiver is located at $\boldsymbol{l}_{\rm r} = [4\ 4\ 1]^T$ m and looks upwards, i.e., the orientation vector is given by $\boldsymbol{n}_{\rm r} = [0\ 0\ 1]^T$.

In the following subsections, the CRLBs and the performance of the direct position (DP) estimators and the two-step (TS) estimators are evaluated for both synchronous and asynchronous VLP systems. The CRLBs are computed based on Proposition 1 and Proposition 3, and the DP estimators are implemented via (19) and (44) for the synchronous and asynchronous cases, respectively. Also, the two-step (TS) estimator in the synchronous scenario is obtained via (21), (24), and (28). Furthermore, the minimum mean absolute error (MMAE) estimator in [7] is implemented to compare the proposed estimators with the current state-of-the-art.[8,9]

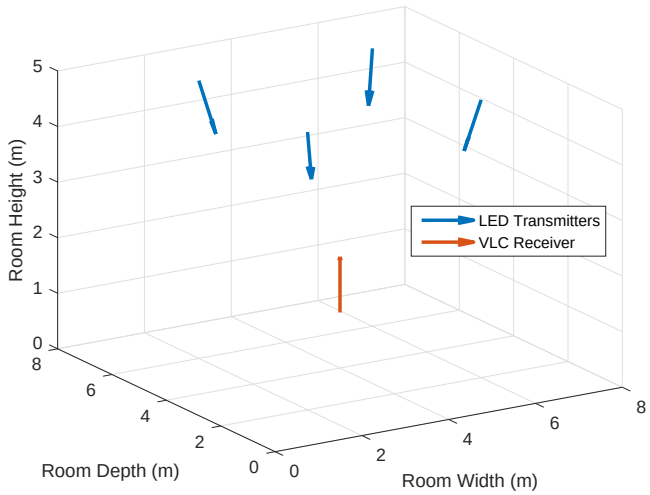

Fig. 1. VLP system configuration in the simulations, where wall reflections are omitted by assuming an LOS scenario.

A. Theoretical Accuracy Limits over the Room

In order to observe the localization performance throughout the entire room, the CRLBs for the synchronous and asynchronous VLP systems are computed as the VLC receiver moves inside the room and the resulting contour plots are shown in Fig. 2 and Fig. 3, respectively. The CRLBs are obtained for position estimation of a VLC receiver with a fixed height $l_{{\rm r},3} = 1\,$m, which is moved along the $x-y$ plane over the room. As noted from Fig. 2 and Fig. 3, the localization performance decreases as the receiver moves away from the center of the room, which is an expected outcome since that movement leads to an increase in the distance, the incidence angle, and the irradiation angle between the VLC receiver and the LED transmitters, thereby reducing the signal strength, as implied by the Lambertian formula in (3). In addition, the level of increase in the CRLB from the center to the corners is much higher in the asynchronous case than that in the synchronous case as the TOA information can be effectively exploited to facilitate the localization process at the room corners, where the RSS information becomes less useful. Furthermore, the CRLBs are significantly lower in the synchronous case than

[6]Since the direct and two-step estimators in asynchronous systems are equivalent for $E^i_3 = 0$ via Proposition 4, the computational complexity analysis is carried out only for the direct estimator in (44). When $E^i_3 \neq 0$, the estimators in (44) and (46) still have the same complexity as the computation of E^i_3 requires constant time, i.e., of complexity $\mathcal{O}(1)$.

[7]For example, when $\theta_i = 180°$ and $\phi_i = 0°$, the LED orientation vector is directed downwards, i.e., $\boldsymbol{n}^i_{\rm t} = [0\ 0\ -1]$.

[8]Since the localization algorithm in [7] depends on the assumption of a perpendicular LED orientation, implementing it directly for the configuration of Fig. 1 would yield poor localization performance. To perform a fair evaluation of the algorithm in [7], we express the irradiation and the incidence angles in [7, Eq. 10] as a function of positions and orientations as in (3), which makes the algorithm applicable for Fig. 1.

[9]For the implementation of all the estimators in this work, the search interval in all the dimensions is taken to be $[-100\ 100]\,$m.

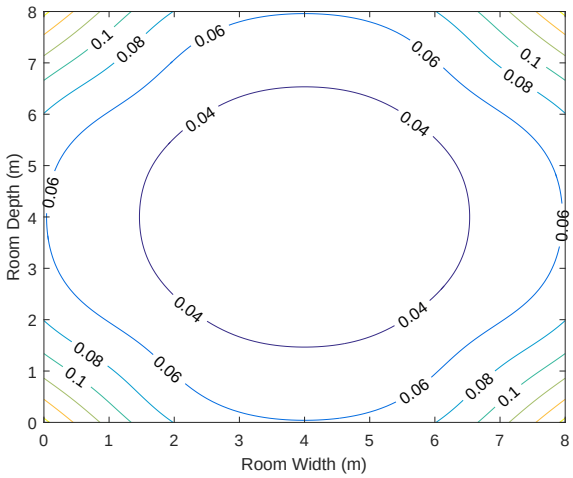

Fig. 2. CRLB (in meters) for a synchronous VLP system as the VLC receiver moves inside the room, where $T_s = 0.1\,\text{ms}$, $f_c = 100\,\text{MHz}$, and $A = 100\,\text{mW}$.

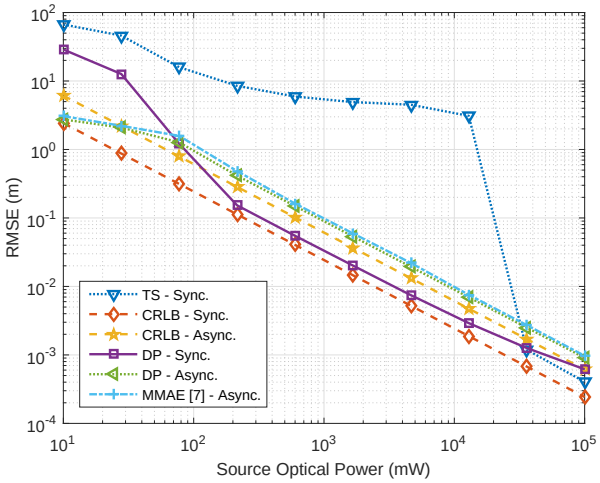

Fig. 4. CRLBs and RMSEs of the estimators for synchronous and asynchronous VLP systems versus source optical power, where $T_s = 1\,\mu\text{s}$ and $f_c = 100\,\text{MHz}$.

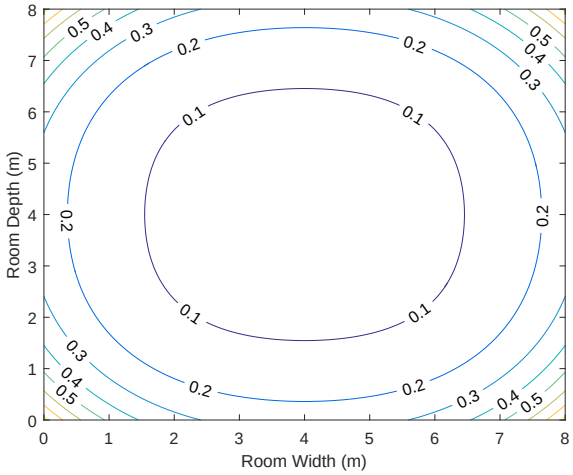

Fig. 3. CRLB (in meters) for an asynchronous VLP system as the VLC receiver moves inside the room, where $T_s = 0.1\,\text{ms}$, $f_c = 100\,\text{MHz}$, and $A = 100\,\text{mW}$.

those in the asynchronous case as the carrier frequency is quite high, which is in agreement with Remark 2.

B. Performance of Direct and Two-Step Estimators with Respect to Optical Power

In this subsection, the root mean-squared errors (RMSEs) corresponding to the proposed DP and TS estimators, the MMAE estimator in [7], and the CRLBs are plotted with respect to the source optical power, A, for $f_c = 100\,\text{MHz}$ and $f_c = 10\,\text{MHz}$ in Fig. 4 and Fig. 5, respectively.[10] First, it is seen that the DP approach can provide significant performance improvements over the TS approach for synchronous scenarios, especially in the low-to-medium SNR region (about 4.5 m improvement for $A = 4.64$ W and $f_c = 100\,\text{MHz}$). Also, it can be inferred from the figures that the utilization of the time delay information in the synchronous DP estimator leads to considerable performance gains as compared to its asynchronous counterpart (0.26 m gain for $A = 215$ mW and $f_c = 100\,\text{MHz}$). It is important to highlight that performance enhancement due to synchronism becomes larger as the center frequency increases, in compliance with Remark 2. Next, it is observed that the performance of the DP estimator in the synchronous case converges to that of the TS estimator at high SNR values (at high source optical powers) since the benefits of direct positioning get negligible as the SNR increases, which complies with Proposition 2 and Remark 1. Hence, the extra information acquired by utilizing the entire received signal for localization as opposed to using a set of intermediate measurements (i.e., TOA and RSS estimates) leads to higher performance gains in low-to-medium SNR regimes. Therefore, it is deduced that the two-step positioning approach in the synchronous VLP systems is best suited for high SNR scenarios, where direct and two-step positioning achieve similar localization performance with the latter method requiring reduced computational resources, as explored in Section III-D. Moreover, the proposed DP approach outperforms the algorithm in [7] at all SNR levels and center frequencies.

C. Performance of Direct and Two-Step Estimators with Respect to VLC Receiver Coordinates

In this subsection, theoretical bounds and estimator performances are investigated along a horizontal path inside the room. In Fig. 6 and Fig. 7, the CRLBs and the RMSEs of the DP and TS estimators and the algorithm in [7] are illustrated for $f_c = 100\,\text{MHz}$ and $f_c = 10\,\text{MHz}$, respectively, as the VLC receiver moves on a straight line starting from $[4\ 0\ 1]\,\text{m}$ and ending at $[4\ 8\ 1]\,\text{m}$ inside the room. It is observed that the estimator performances tend to decrease as the receiver moves towards the edge of the room, as indicated by the Lambertian formula in (3). In addition, the TS estimator for

[10] The estimators can achieve lower RMSEs than the corresponding CRLBs at low SNRs since the theoretically infinite search space for the unknown parameter is confined to a finite region when implementing the estimators due to practical concerns, as described in Footnote 9.

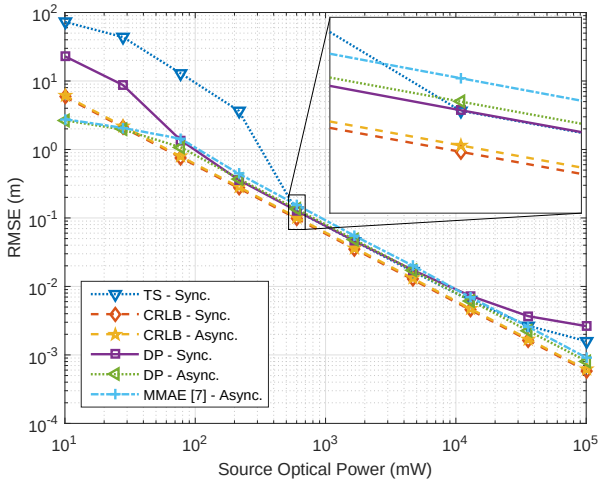

Fig. 5. CRLBs and RMSEs of the estimators for synchronous and asynchronous VLP systems versus source optical power, where $T_s = 1\,\mu$s and $f_c = 10\,$MHz.

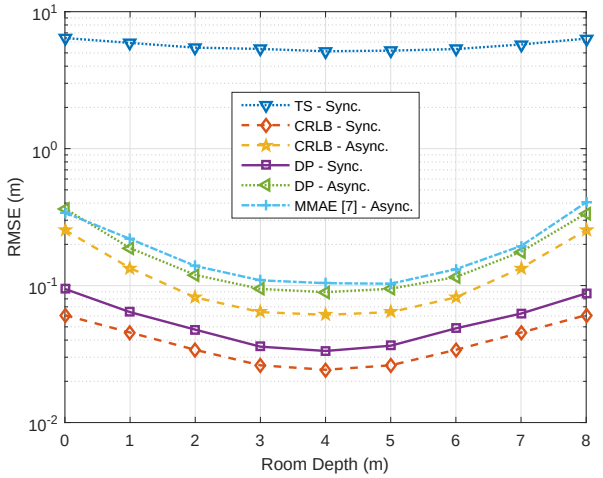

Fig. 6. CRLBs and RMSEs of the estimators for synchronous and asynchronous VLP systems as the VLC receiver moves on a straight line in the room, where $T_s = 1\,\mu$s, $A = 1\,$W and $f_c = 100\,$MHz.

$f_c = 10\,$MHz exhibits significantly higher performance than that for $f_c = 100\,$MHz. The reason for this behaviour is that the first-step TOA estimation errors are weighted by the inverse of the corresponding analytical CRLBs in (28), which do not provide tight bounds at low SNRs for the ML estimates of the TOA in the first step in (21). Furthermore, the figures show that the proposed direct scheme in the asynchronous case attains higher performance than the localization algorithm in [7] at most of the locations in the room.

D. Performance of Direct and Two-Step Estimators in the Presence of Model Uncertainties

In this part, the performances of the proposed direct and two-step estimators are evaluated in the presence of uncertainties related to the attenuation model for visible light channels, i.e., the Lambertian model in (3). Since the knowledge of model-related parameters is imperfect in practical localization

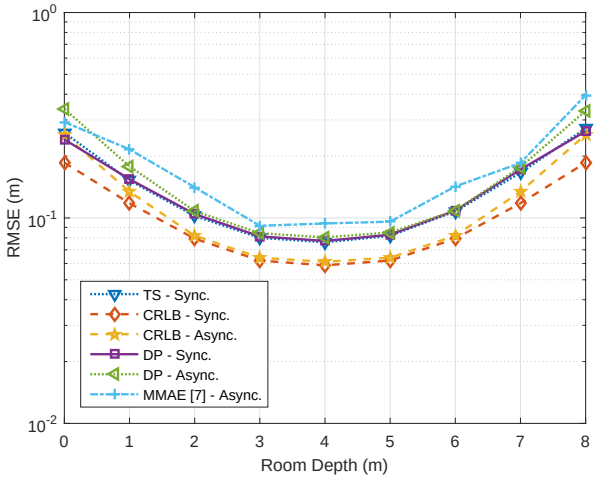

Fig. 7. CRLBs and RMSEs of the estimators for synchronous and asynchronous VLP systems as the VLC receiver moves on a straight line in the room, where $T_s = 1\,\mu$s, $A = 1\,$W and $f_c = 10\,$MHz.

scenarios, it is important to assess the localization performance under various degrees of uncertainty, which is useful to reveal the robustness of the proposed algorithms against parameter/model mismatches.

1) Performance with Respect to Uncertainty in Lambertian Order: First, we consider the case in which the Lambertian order m_i in (3) is known with a certain degree of uncertainty. To that aim, a measured (estimated) value $\hat{m}_i$, which does not perfectly match the true value m_i, is used in the proposed DP and TS estimators and in the localization algorithm in [7]. In the simulations, m_i is set to 1 and $\hat{m}_i$ is varied over the interval $[0.75\ 1.25]$ for $i \in \{1, \ldots, N_{\mathrm{L}}\}$. Fig. 8 and Fig. 9 show the localization performance of the considered approaches with respect to the measured value of the Lambertian order for $f_c = 100\,$MHz and $f_c = 10\,$MHz, respectively. It is observed from the figures that the localization performance deteriorates as the measured/estimated Lambertian order deviates from the true value, as expected. In addition, it is noted that the synchronous DP estimator is more robust to Lambertian order mismatches than the asynchronous algorithms. The reason is that the TOA information, which is independent of the Lambertian order (see (2)), becomes the dominant factor affecting the localization performance as the uncertainty in the Lambertian order grows, hindering the effective use of the RSS information (see (3)). Hence, the robustness of the synchronous positioning against uncertainties in the Lambertian order is more evident at high center frequencies with an increase in the accuracy of TOA information [19], which can also be observed by comparing Fig. 8 and Fig. 9. Moreover, in the asynchronous case, the proposed algorithm performs slightly better than that in [7] for various degrees of uncertainty.

2) Performance with Respect to Uncertainty in Transmission Model: Next, we investigate the estimator performances in the presence of uncertainty in the overall transmission model in (3). As in [50], we assume a multiplicative uncertainty model that represents all the individual uncertainties embedded in (3) (e.g., $\boldsymbol{l}_{\mathrm{t}}^i$, $\boldsymbol{n}_{\mathrm{t}}^i$, $\boldsymbol{n}_{\mathrm{r}}$, and m_i) in the form of

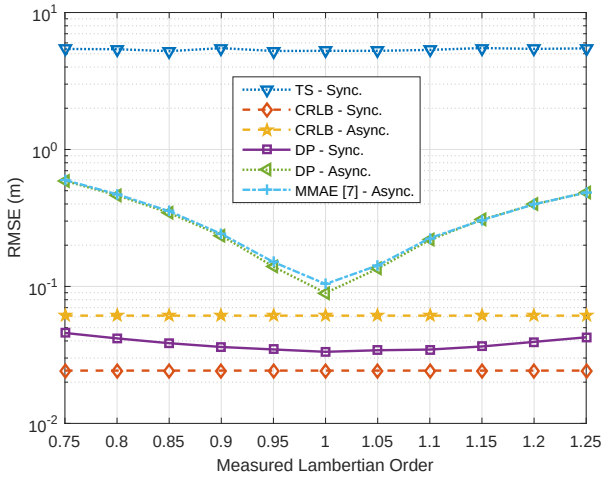

Fig. 8. CRLBs and RMSEs of the estimators for synchronous and asynchronous VLP systems under imperfect knowledge of Lambertian order, where true Lambertian order is 1, $T_s = 1\,\mu$s, $A = 1\,$W, and $f_c = 100\,$MHz.

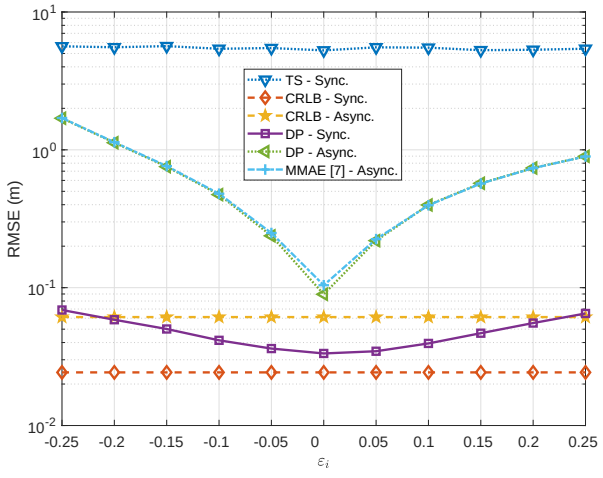

Fig. 10. CRLBs and RMSEs of the estimators for synchronous and asynchronous VLP systems under mismatched transmission model, where $T_s = 1\,\mu$s, $A = 1\,$W, and $f_c = 100\,$MHz.

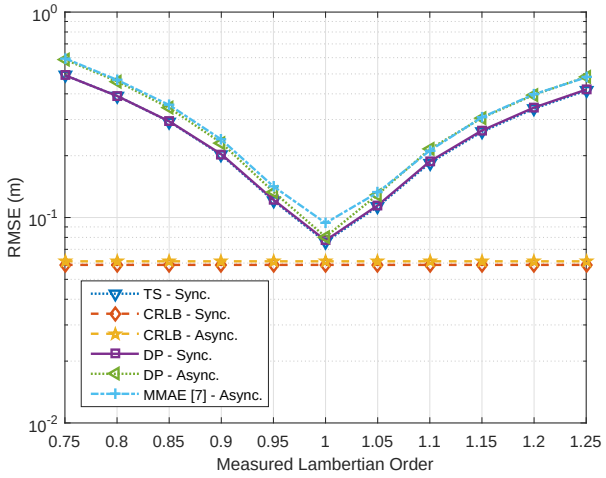

Fig. 9. CRLBs and RMSEs of the estimators for synchronous and asynchronous VLP systems under imperfect knowledge of Lambertian order, where true Lambertian order is 1, $T_s = 1\,\mu$s, $A = 1\,$W, and $f_c = 10\,$MHz.

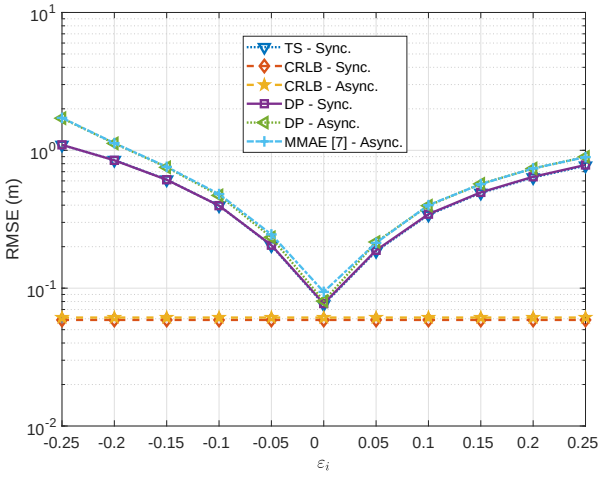

Fig. 11. CRLBs and RMSEs of the estimators for synchronous and asynchronous VLP systems under mismatched transmission model, where $T_s = 1\,\mu$s, $A = 1\,$W, and $f_c = 10\,$MHz.

a multiplication of the true transmission model. More specifically, the position estimation is performed by considering the following transmission model:

$$\alpha_i^{\text{meas}} = (1 + \varepsilon_i)\alpha_i,\ i = 1, \ldots, N_{\text{L}} \tag{54}$$

where α_i is as defined in (3) and $\varepsilon_i \in \left[\varepsilon_i^{\min}, \varepsilon_i^{\max}\right]$ specifies the degree of mismatch between the true and the estimated transmission models. In Fig. 10 and Fig. 11, the RMSEs of the estimators are plotted against the degree of uncertainty, ε_i, for $f_c = 100\,$MHz and $f_c = 10\,$MHz, respectively, where $\varepsilon_i^{\min} = -0.25$ and $\varepsilon_i^{\max} = 0.25$ for $i = 1, \ldots, N_{\text{L}}$. As observed from the figures, the localization performance curves with respect to the degree of uncertainty in the transmission model exhibit similar trends to those for the case of uncertainty in the Lambertian order.

E. Special Case: Two-Dimensional Localization

In this part, we investigate the two-dimensional localization performance of the proposed estimators and perform comparisons with the trilateration method, which is one of the most commonly used methods in two-dimensional visible light localization. Specifically, we implement the linear least-squares (LLS) based trilateration algorithm in [43] via Eqs. (6), (7), (9), and (17) therein.[11] For the CRLB computations and algorithm implementations, we assume that the receiver height is known and perform two-dimensional position estimation accordingly. We carry out two experiments to assess the relative performance of the proposed estimators, the MMAE estimator in [7], and the LLS based trilateration algorithm in

[11]For the implementation in [43], the Lambertian modeling in (12) and (13) is used. The parameters in (17) are taken as $A = 1$, $h = 4\,$m, and $CS = 6\sqrt{2}\,$m in accordance with the configuration in Fig. 1.

[43]. In the experiments, the polar and azimuth angles of the LEDs are set to be $(\theta_i, \phi_i) = (180°, 0°)$ for $i = 1, \ldots, N_{\mathrm{L}}$, i.e., the LEDs are facing downwards.

1) Performance with Respect to Optical Power: In Fig. 12, we present the RMSE performance of the proposed DP and TS algorithms, the algorithm in [7], and the LLS based trilateration algorithm in [43] with respect to the optical power for $f_c = 100\,\mathrm{MHz}$ and $\boldsymbol{l}_{\mathrm{r}} = [4\ 6\ 1]\,\mathrm{m}$. It is observed that, in the asynchronous case, the proposed direct estimator is able to outperform both the MMAE estimator in [7] and the trilateration algorithm in [43] at almost all SNR levels. For instance, for $A = 215\,\mathrm{mW}$, the improvements in localization performance achieved by the proposed DP method are about $10\,\mathrm{cm}$ and $40\,\mathrm{cm}$ as compared to the positioning methods in [7] and [43], respectively. In addition, we note that the synchronous DP estimator outperforms all the asynchronous estimators by using the time delay information. Moreover, the proposed synchronous TS estimator converges to the CRLB at high SNR regime, which results from its asymptotic optimality property, as shown in Proposition 2 and Remark 1. Therefore, similarly to Fig. 4 and Fig. 5 in Section V-B, Fig. 12 illustrates the trade-off between direct and two-step positioning in terms of localization performance and computational complexity at different SNR regimes.

2) Performance with Respect to VLC Receiver Coordinates: Fig. 13 depicts the two-dimensional localization performance as the VLC receiver moves along the horizontal line starting from $[4\ 0\ 1]\,\mathrm{m}$ and ending at $[4\ 8\ 1]\,\mathrm{m}$ for $f_c = 100\,\mathrm{MHz}$. It is observed that the proposed ML-based direct positioning technique can attain higher localization performance than the algorithms in [7] and [43] at all the locations along the line. Also, the performance of the algorithm in [43] gets worse as the receiver moves away from the center of the room towards the edges. This is because the trilateration-based method in [43] is a suboptimal three-step approach that first estimates the distances to the LEDs by using the RSS observations, then adjusts the estimated distances via normalization and finally employs the LLS method based on the normalized distances. As the symmetry is reduced at the room edges, the normalization method applied in [43] (see (6) and (7) therein), which assigns the same normalizing constant and factor to distance estimates from different LEDs, becomes less accurate. The proposed ML-based estimator, on the other hand, achieves RMSE levels close to the CRLB at all positions along the line and therefore leads to a substantial improvement in localization performance as compared to the method in [43] (about $63\,\mathrm{cm}$ improvement for $\boldsymbol{l}_{\mathrm{r}} = [4\ 8\ 1]\,\mathrm{m}$).

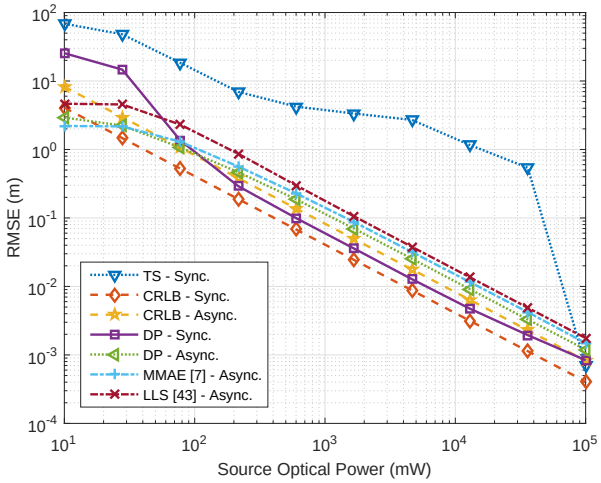

Fig. 12. CRLBs and RMSEs of the estimators for two-dimensional localization in synchronous and asynchronous VLP systems with respect to source optical power, where $T_s = 1\,\mu\mathrm{s}$ and $f_c = 100\,\mathrm{MHz}$.

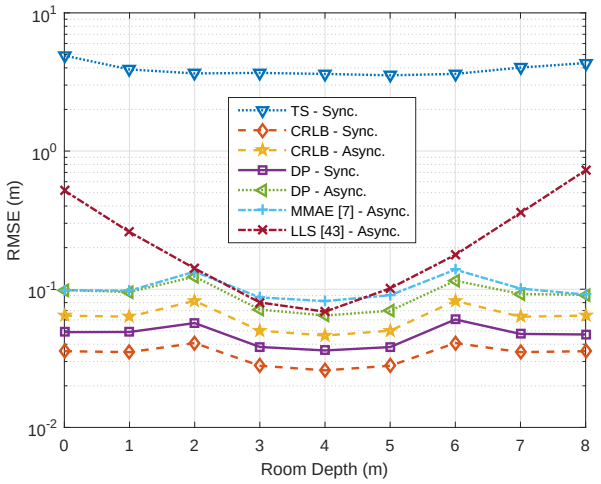

Fig. 13. CRLBs and RMSEs of the estimators for two-dimensional localization in synchronous and asynchronous VLP systems with respect to room depth, where $T_s = 1\,\mu\mathrm{s}$, $A = 1\,\mathrm{W}$ and $f_c = 100\,\mathrm{MHz}$.

VI. Concluding Remarks

In this study, direct and two-step positioning paradigms have been investigated for VLP systems. In particular, the CRLBs and the direct and two-step position estimators are derived in synchronous and asynchronous VLP systems. The proposed CRLB expressions exploit the entire observation signal at the VLC receiver and can be applied to any VLP system in which the LED transmitters and the VLC receiver can have arbitrary orientations. The CRLB on the localization accuracy of synchronous VLP systems that utilize both TOA and RSS information has been derived for the first time in the literature. In addition, the CRLB presented for the asynchronous case generalizes an expression available in the literature to any type of transmitted pulses. Comparative analysis on the performance of synchronous and asynchronous systems has indicated that the advantage of synchronous positioning becomes more noticeable as the effective bandwidth of the transmitted pulse increases. Furthermore, in order to explore the relationship between direct and two-step positioning approaches, the conditions of (asymptotic) equivalence of these two approaches have been identified. It has been proved that the two-step estimator converges to the direct estimator at high SNRs for synchronous systems, whereas the two estimators are equivalent for asynchronous systems at all SNRs for practical pulse shapes. Therefore, the benefits of direct positioning on localization accuracy can be significant for synchronous systems at low-to-medium

SNRs. Furthermore, the computational complexities of the proposed approaches have been presented to demonstrate the trade-off between implementation complexity and localization accuracy. Various numerical examples have been provided to illustrate the effects of direct positioning on the performance of VLP systems and to present a comparative evaluation of synchronous and asynchronous scenarios. As future work, the effects of synchronization errors can be analyzed for three-dimensional localization in VLP systems. In particular, in the presence of significant synchronization errors, it may not be useful to utilize TOA measurements in addition to RSS measurements for localization purposes. Therefore, quantifying the information that can be extracted from TOA measurements with synchronization errors is an important issue. As another direction for future work, VLP in the presence of model and parameter uncertainty can be considered with the aim of designing robust position estimators.

APPENDIX

A. Proof of Lemma 1

Consider the estimation of τ_i and α_i based on the received signal from the ith LED transmitter, i.e., $r_i(t)$ in (1). The log-likelihood function for $r_i(t)$ is given by

$$\Lambda_i(\tau_i,\alpha_i) = k_i - \frac{1}{2\sigma^2}\int_{T_{1,i}}^{T_{2,i}} \left(r_i(t) - \alpha_i R_p\, s_i(t-\tau_i)\right)^2 dt \tag{55}$$

where k_i is a constant that does not depend on α_i and τ_i (cf. (4)). The FIM for (τ_i,α_i) can be expressed based on (6) as follows:

$$\mathbf{J}(\tau_i,\alpha_i) = \begin{bmatrix} \mathrm{E}\left\{\left(\frac{\partial\Lambda_i(\tau_i,\alpha_i)}{\partial\tau_i}\right)^2\right\} & \mathrm{E}\left\{\frac{\partial\Lambda_i(\tau_i,\alpha_i)}{\partial\tau_i}\frac{\partial\Lambda_i(\tau_i,\alpha_i)}{\partial\alpha_i}\right\} \\ \mathrm{E}\left\{\frac{\partial\Lambda_i(\tau_i,\alpha_i)}{\partial\alpha_i}\frac{\partial\Lambda_i(\tau_i,\alpha_i)}{\partial\tau_i}\right\} & \mathrm{E}\left\{\left(\frac{\partial\Lambda_i(\tau_i,\alpha_i)}{\partial\alpha_i}\right)^2\right\} \end{bmatrix} \tag{56}$$

the elements of which can be computed from (55) as

$$[\mathbf{J}(\tau_i,\alpha_i)]_{11} = \frac{\alpha_i^2 R_p^2 E_1^i}{\sigma^2} \tag{57}$$

$$[\mathbf{J}(\tau_i,\alpha_i)]_{22} = \frac{R_p^2 E_2^i}{\sigma^2} \tag{58}$$

$$[\mathbf{J}(\tau_i,\alpha_i)]_{12} = [\mathbf{J}(\tau_i,\alpha_i)]_{21} = \frac{-\alpha_i R_p^2 E_3^i}{\sigma^2} \tag{59}$$

where E_1^i, E_2^i, and E_3^i are as defined in (10), (11), and (12), respectively. Since $E_3^i = 0$ for $i = 1,\ldots,N_{\mathrm{L}}$ as stated in the lemma, the FIM in (56) can be expressed from (57)–(59) as

$$\mathbf{J}(\tau_i,\alpha_i) = \begin{bmatrix} \frac{R_p^2\alpha_i^2 E_1^i}{\sigma^2} & 0 \\ 0 & \frac{R_p^2 E_2^i}{\sigma^2} \end{bmatrix}. \tag{60}$$

As studied in [49], [51], the ML estimates for τ_i and α_i can be approximated, at high SNRs, by a Gaussian random vector, where the mean of each component is equal to the true value of the parameter and the covariance matrix is given by the inverse of the FIM. Hence, at high SNRs, the joint probability distribution of $\hat{\tau}_i$ in (21) and $\hat{\alpha}_i$ in (24) can approximately be expressed as

$$\begin{bmatrix}\hat{\tau}_i \\ \hat{\alpha}_i\end{bmatrix} \sim \mathcal{N}\left(\begin{bmatrix}\tau_i \\ \alpha_i\end{bmatrix}, \begin{bmatrix}\frac{\sigma^2}{R_p^2\alpha_i^2 E_1^i} & 0 \\ 0 & \frac{\sigma^2}{R_p^2 E_2^i}\end{bmatrix}\right) \tag{61}$$

where $\mathcal{N}(\boldsymbol{\mu},\boldsymbol{\Sigma})$ denotes Gaussian distribution with mean vector $\boldsymbol{\mu}$ and covariance matrix $\boldsymbol{\Sigma}$. Hence, $\hat{\tau}_i$ and $\hat{\alpha}_i$ are independent Gaussian random variables as specified by (25) and (26) in the lemma. In addition, since the noise $\eta_i(t)$ in the received signal, $r_i(t)$, is independent for different LED transmitters (see (1)), the noise components in the ML estimates $\hat{\tau}_i$ and $\hat{\alpha}_i$ are also independent for different transmitters. Hence, the noise components in (25) and (26) are independent as specified in the lemma. ■

B. Derivation of (27)

Based on Lemma 1, the joint distribution of $\hat{\tau}_i$ and $\hat{\alpha}_i$ can be specified as in (61), and $\hat{\tau}_i$ and $\hat{\tau}_j$ ($\hat{\alpha}_i$ and $\hat{\alpha}_j$) are conditionally independent for a given value of $\boldsymbol{l}_{\mathrm{r}}$ whenever $i \neq j$. Therefore, the joint probability density function of $\{\hat{\tau}_i,\hat{\alpha}_i\}_{i=1}^{N_{\mathrm{L}}}$ for a given value of $\boldsymbol{l}_{\mathrm{r}}$; that is, the likelihood function for $\boldsymbol{l}_{\mathrm{r}}$, is obtained as follows:

$$\begin{aligned} p(\hat{\boldsymbol{\tau}},\hat{\boldsymbol{\alpha}}|\boldsymbol{l}_{\mathrm{r}}) = &\prod_{i=1}^{N_{\mathrm{L}}} \frac{R_p\alpha_i\sqrt{E_1^i}}{\sqrt{2\pi}\,\sigma}\exp\left\{-\frac{R_p^2\alpha_i^2E_1^i}{2\sigma^2}(\hat{\tau}_i-\tau_i)^2\right\} \\ &\times\prod_{i=1}^{N_{\mathrm{L}}} \frac{R_p\sqrt{E_2^i}}{\sqrt{2\pi}\,\sigma}\exp\left\{-\frac{R_p^2E_2^i}{2\sigma^2}(\hat{\alpha}_i-\alpha_i)^2\right\} \end{aligned} \tag{62}$$

where $\hat{\boldsymbol{\tau}} = (\hat{\tau}_1,\ldots,\tau_{\hat{N}_{\mathrm{L}}})$ and $\hat{\boldsymbol{\alpha}} = (\hat{\alpha}_1,\ldots,\alpha_{\hat{N}_{\mathrm{L}}})$. From (62), the log-likelihood function can be expressed as

$$\begin{aligned} \tilde{\Lambda}(\boldsymbol{l}_{\mathrm{r}}) = &\tilde{k} + \sum_{i=1}^{N_{\mathrm{L}}}\log\alpha_i \\ &- \frac{R_p^2}{2\sigma^2}\sum_{i=1}^{N_{\mathrm{L}}}\left(\alpha_i^2E_1^i(\hat{\tau}_i-\tau_i)^2 + E_2^i(\hat{\alpha}_i-\alpha_i)^2\right) \end{aligned} \tag{63}$$

where $\tilde{k}$ is a constant that is independent of α_i's and τ_i's. Hence, the ML estimate for $\boldsymbol{l}_{\mathrm{r}}$ can be obtained from (63) as in (27). ■

C. Proof of Proposition 2

The derivative of the log-likelihood function in (63) with respect to the kth parameter of the unknown parameter vector $\boldsymbol{l}_{\mathrm{r}}$ is computed as

$$\begin{aligned} \frac{\partial\tilde{\Lambda}(\boldsymbol{l}_{\mathrm{r}})}{\partial l_{\mathrm{r},k}} = \sum_{i=1}^{N_{\mathrm{L}}}\Bigg(&\frac{1}{\alpha_i}\frac{\partial\alpha_i}{\partial l_{\mathrm{r},k}} + \frac{(\hat{\alpha}_i-\alpha_i)R_p^2E_2^i}{\sigma^2}\frac{\partial\alpha_i}{\partial l_{\mathrm{r},k}} \\ &+ \frac{(\hat{\tau}_i-\tau_i)\alpha_i^2R_p^2E_1^i}{\sigma^2}\frac{\partial\tau_i}{\partial l_{\mathrm{r},k}} \\ &- \frac{(\hat{\tau}_i-\tau_i)^2\alpha_iR_p^2E_1^i}{\sigma^2}\frac{\partial\alpha_i}{\partial l_{\mathrm{r},k}}\Bigg) \end{aligned} \tag{64}$$

for $k \in \{1,2,3\}$. Using the formula in (6) with the expression in (64), the (k_1,k_2)th entry of the FIM can be obtained after some manipulation as

$$[\mathbf{J}_{\mathrm{TS,syn}}]_{k_1,k_2} = \frac{R_p^2}{\sigma^2}\sum_{i=1}^{N_{\mathrm{L}}}\left(\left(1+\frac{2\sigma^2}{\alpha_i^2 R_p^2 E_2^i}\right)E_2^i \frac{\partial \alpha_i}{\partial l_{\mathrm{r},k_1}}\frac{\partial \alpha_i}{\partial l_{\mathrm{r},k_2}} + E_1^i \alpha_i^2 \frac{\partial \tau_i}{\partial l_{\mathrm{r},k_1}}\frac{\partial \tau_i}{\partial l_{\mathrm{r},k_2}}\right) \quad (65)$$

for $k_1, k_2 \in \{1,2,3\}$. By invoking the assumption of high SNRs in Lemma 1 ($\alpha_i^2 R_p^2 E_2^i \gg \sigma^2$), the FIM for the unknown receiver location $\boldsymbol{l}_{\mathrm{r}}$ can be obtained as in (30). ■

D. Derivation of (47)

Consider the estimation of τ_i and α_i from $r_i(t)$ in (1). As derived in Appendix A, the FIM can be expressed, from (56)–(59), as

$$\mathbf{J}(\tau_i,\alpha_i) = \begin{bmatrix} \frac{\alpha_i^2 R_p^2 E_1^i}{\sigma^2} & \frac{-\alpha_i R_p^2 E_3^i}{\sigma^2} \\ \frac{-\alpha_i R_p^2 E_3^i}{\sigma^2} & \frac{R_p^2 E_2^i}{\sigma^2} \end{bmatrix}. \quad (66)$$

Then, the CRLB on estimating α_i can be obtained as

$$\mathrm{E}\{(\hat{\alpha}_i - \alpha_i)^2\} \geq [\mathbf{J}^{-1}(\tau_i,\alpha_i)]_{2,2} = \frac{E_1^i \sigma^2 / R_p^2}{E_1^i E_2^i - (E_3^i)^2} \quad (67)$$

Hence, the weighting coefficient in (47) is inversely proportional to the CRLB for estimating α_i from $r_i(t)$. ■

Acknowledgments: *The authors would like to thank Mr. Ahmet Dundar Sezer from Bilkent University and the anonymous reviewers for their valuable comments and suggestions.*

REFERENCES

[1] H. Burchardt, N. Serafimovski, D. Tsonev, S. Videv, and H. Haas, "VLC: Beyond point-to-point communication," *IEEE Communications Magazine*, vol. 52, no. 7, pp. 98–105, July 2014.

[2] P. H. Pathak, X. Feng, P. Hu, and P. Mohapatra, "Visible light communication, networking, and sensing: A survey, potential and challenges," *IEEE Communications Surveys Tutorials*, vol. 17, no. 4, pp. 2047–2077, Fourthquarter 2015.

[3] S. Rajagopal, R. D. Roberts, and S. K. Lim, "IEEE 802.15.7 visible light communication: modulation schemes and dimming support," *IEEE Communications Magazine*, vol. 50, no. 3, pp. 72–82, Mar. 2012.

[4] J. Armstrong, Y. Sekercioglu, and A. Neild, "Visible light positioning: A roadmap for international standardization," *IEEE Communications Magazine*, vol. 51, no. 12, pp. 68–73, Dec. 2013.

[5] T. Wang, Y. Sekercioglu, A. Neild, and J. Armstrong, "Position accuracy of time-of-arrival based ranging using visible light with application in indoor localization systems," *Journal of Lightwave Technology*, vol. 31, no. 20, pp. 3302–3308, Oct. 2013.

[6] X. Zhang, J. Duan, Y. Fu, and A. Shi, "Theoretical accuracy analysis of indoor visible light communication positioning system based on received signal strength indicator," *Journal of Lightwave Technology*, vol. 32, no. 21, pp. 4180–4186, Nov. 2014.

[7] L. Li, P. Hu, C. Peng, G. Shen, and F. Zhao, "Epsilon: A visible light based positioning system," in *11th USENIX Symposium on Networked Systems Design and Implementation (NSDI)*, Seattle, WA, Apr. 2014, pp. 331–343.

[8] D. Ganti, W. Zhang, and M. Kavehrad, "VLC-based indoor positioning system with tracking capability using Kalman and particle filters," in *IEEE International Conference on Consumer Electronics (ICCE)*, Jan. 2014, pp. 476–477.

[9] Y. Eroglu, I. Guvenc, N. Pala, and M. Yuksel, "AOA-based localization and tracking in multi-element VLC systems," in *IEEE 16th Annual Wireless and Microwave Technology Conference (WAMICON)*, Apr. 2015.

[10] S. Schmid, T. Richner, S. Mangold, and T. R. Gross, "Enlighting: An indoor visible light communication system based on networked light bulbs," in *2016 13th Annual IEEE International Conference on Sensing, Communication, and Networking (SECON)*, June 2016, pp. 1–9.

[11] B. Turan, O. Narmanlioglu, S. C. Ergen, and M. Uysal, "Physical layer implementation of standard compliant vehicular VLC," in *IEEE 84th Vehicular Technology Conference*, Sep. 2016.

[12] B. Lin, Z. Ghassemlooy, C. Lin, X. Tang, Y. Li, and S. Zhang, "An indoor visible light positioning system based on optical camera communications," *IEEE Photonics Technology Letters*, vol. 29, no. 7, pp. 579–582, April 2017.

[13] Q.-L. Li, J.-Y. Wang, T. Huang, and Y. Wang, "Three-dimensional indoor visible light positioning system with a single transmitter and a single tilted receiver," *Optical Engineering*, vol. 55, no. 10, p. 106103, 2016.

[14] Y. Hu, Y. Xiong, W. Huang, X. Y. Li, Y. Zhang, X. Mao, P. Yang, and C. Wang, "Lightitude: Indoor positioning using ubiquitous visible lights and COTS devices," in *2015 IEEE 35th International Conference on Distributed Computing Systems*, June 2015, pp. 732–733.

[15] M. Aminikashani, W. Gu, and M. Kavehrad, "Indoor positioning with OFDM visible light communications," in *2016 13th IEEE Annual Consumer Communications Networking Conference (CCNC)*, Jan 2016, pp. 505–510.

[16] S.-H. Yang, E.-M. Jung, and S.-K. Han, "Indoor location estimation based on LED visible light communication using multiple optical receivers," *IEEE Communications Letters*, vol. 17, no. 9, pp. 1834–1837, Sep. 2013.

[17] S.-Y. Jung, S. Hann, and C.-S. Park, "TDOA-based optical wireless indoor localization using LED ceiling lamps," *IEEE Transactions on Consumer Electronics*, vol. 57, no. 4, pp. 1592–1597, Nov. 2011.

[18] W. Zhang, M. I. S. Chowdhury, and M. Kavehrad, "Asynchronous indoor positioning system based on visible light communications," *Optical Engineering*, vol. 53, no. 4, pp. 045 105–1–045 105–9, 2014.

[19] Z. Sahinoglu, S. Gezici, and I. Guvenc, *Ultra-Wideband Positioning Systems: Theoretical Limits, Ranging Algorithms, and Protocols*. New York, Cambridge University Press, 2008.

[20] C. Wang, L. Wang, X. Chi, S. Liu, W. Shi, and J. Deng, "The research of indoor positioning based on visible light communication," *China Communications*, vol. 12, no. 8, pp. 85–92, August 2015.

[21] W. Xu, J. Wang, H. Shen, H. Zhang, and X. You, "Indoor positioning for multiphotodiode device using visible-light communications," *IEEE Photonics Journal*, vol. 8, no. 1, pp. 1–11, Feb 2016.

[22] S.-H. Yang, H.-S. Kim, Y.-H. Son, and S.-K. Han, "Three-dimensional visible light indoor localization using AOA and RSS with multiple optical receivers," *Journal of Lightwave Technology*, vol. 32, no. 14, pp. 2480–2485, July 2014.

[23] A. Sahin, Y. S. Eroglu, I. Guvenc, N. Pala, and M. Yuksel, "Hybrid 3-D localization for visible light communication systems," *Journal of Lightwave Technology*, vol. 33, no. 22, pp. 4589–4599, Nov. 2015.

[24] G. B. Prince and T. D. C. Little, "Latency constrained device positioning using a visible light communication two-phase received signal strength - angle of arrival algorithm," in *2015 International Conference on Indoor Positioning and Indoor Navigation (IPIN)*, Oct. 2015, pp. 1–7.

[25] M. F. Keskin and S. Gezici, "Comparative theoretical analysis of distance estimation in visible light positioning systems," *Journal of Lightwave Technology*, vol. 34, no. 3, pp. 854–865, Feb. 2016.

[26] A. J. Weiss and A. Amar, "Direct position determination of multiple radio signals," *EURASIP Journal on Advances in Signal Processing*, vol. 2005, no. 1, pp. 37–49, 2005.

[27] O. Bialer, D. Raphaeli, and A. J. Weiss, "Maximum-likelihood direct position estimation in dense multipath," *IEEE Transactions on Vehicular Technology*, vol. 62, no. 5, pp. 2069–2079, June 2013.

[28] A. J. Weiss, "Direct position determination of narrowband radio frequency transmitters," *IEEE Signal Processing Letters*, vol. 11, no. 5, pp. 513–516, May 2004.

[29] A. Amar and A. J. Weiss, "New asymptotic results on two fundamental approaches to mobile terminal location," in *3rd International Symposium on Communications, Control and Signal Processing*, Mar. 2008, pp. 1320–1323.

[30] P. Closasy, C. Fernndez-Pradesz, and J. A. Fernndez-Rubioy, "Direct position estimation approach outperforms conventional two-steps positioning," in *2009 17th European Signal Processing Conference*, Aug. 2009, pp. 1958–1962.

[31] A. Amar and A. J. Weiss, "Localization of narrowband radio emitters based on doppler frequency shifts," *IEEE Transactions on Signal Processing*, vol. 56, no. 11, pp. 5500–5508, Nov. 2008.

[32] N. Garcia, A. M. Haimovich, M. Coulon, and J. A. Dabin, "High precision TOA-based direct localization of multiple sources

in multipath," *CoRR*, vol. abs/1505.03193, 2015. [Online]. Available: http://arxiv.org/abs/1505.03193
[33] N. Vankayalapati, S. Kay, and Q. Ding, "TDOA based direct positioning maximum likelihood estimator and the Cramer-Rao bound," *IEEE Transactions on Aerospace and Electronic Systems*, vol. 50, no. 3, pp. 1616–1635, July 2014.
[34] N. Garcia, H. Wymeersch, E. G. Larsson, A. M. Haimovich, and M. Coulon, "Direct localization for massive MIMO," *IEEE Transactions on Signal Processing*, vol. 65, no. 10, pp. 2475–2487, May 2017.
[35] O. Bar-Shalom and A. J. Weiss, "Direct positioning of stationary targets using MIMO radar," *Signal Processing*, vol. 91, no. 10, pp. 2345 – 2358, 2011.
[36] L. Tzafri and A. J. Weiss, "High-resolution direct position determination using MVDR," *IEEE Transactions on Wireless Communications*, vol. 15, no. 9, pp. 6449–6461, Sep. 2016.
[37] H. Steendam, T. Q. Wang, and J. Armstrong, "Cramer-Rao bound for indoor visible light positioning using an aperture-based angular-diversity receiver," in *2016 IEEE International Conference on Communications (ICC)*, May 2016, pp. 1–6.
[38] ——, "Theoretical lower bound for indoor visible light positioning using received signal strength measurements and an aperture-based receiver," *Journal of Lightwave Technology*, vol. 35, no. 2, pp. 309–319, Jan. 2017.
[39] G. Kail, P. Maechler, N. Preyss, and A. Burg, "Robust asynchronous indoor localization using led lighting," in *2014 IEEE International Conference on Acoustics, Speech and Signal Processing (ICASSP)*, May 2014, pp. 1866–1870.
[40] M. F. Keskin, E. Gonendik, and S. Gezici, "Improved lower bounds for ranging in synchronous visible light positioning systems," *Journal of Lightwave Technology*, vol. 34, no. 23, pp. 5496–5504, Dec. 2016.
[41] Z. Zheng, L. Liu, and W. Hu, "Accuracy of ranging based on DMT visible light communication for indoor positioning," *IEEE Photonics Technology Letters*, vol. 29, no. 8, pp. 679–682, April 2017.
[42] C. Amini, A. Taherpour, T. Khattab, and S. Gazor, "On the more accurate channel model and positioning based on time-of-arrival for visible light localization," *Optical Engineering*, vol. 56, no. 1, p. 016110, 2017. [Online]. Available: http://dx.doi.org/10.1117/1.OE.56.1.016110
[43] H.-S. Kim, D.-R. Kim, S.-H. Yang, Y.-H. Son, and S.-K. Han, "An indoor visible light communication positioning system using a RF carrier allocation technique," *Journal of Lightwave Technology*, vol. 31, no. 1, pp. 134–144, Jan. 2013.
[44] A. Goldsmith, *Wireless Communications*. Cambridge University Press, 2004.
[45] D. Karunatilaka, F. Zafar, V. Kalavally, and R. Parthiban, "LED based indoor visible light communications: State of the art," *IEEE Communications Surveys & Tutorials*, 2015.
[46] Y. Qi and H. Kobayashi, "Cramér-Rao lower bound for geolocation in non-line-of-sight environment," in *IEEE International Conference on Acoustics, Speech, and Signal Processing (ICASSP)*, vol. 3, May 2002, pp. III–2473–III–2476.
[47] N. Decarli and D. Dardari, "Ziv-Zakai bound for time delay estimation of unknown deterministic signals," in *IEEE International Conference on Acoustics Speech and Signal Processing (ICASSP)*, May 2014, pp. 4673–4677.
[48] H. V. Poor, *An Introduction to Signal Detection and Estimation*. New York: Springer-Verlag, 1994.
[49] Y. Qi, H. Kobayashi, and H. Suda, "On time-of-arrival positioning in a multipath environment," *IEEE Transactions on Vehicular Technology*, vol. 55, no. 5, pp. 1516–1526, Sep. 2006.
[50] A. Mostafa and L. Lampe, "Optimal and robust beamforming for secure transmission in MISO visible-light communication links," *IEEE Transactions on Signal Processing*, vol. 64, no. 24, pp. 6501–6516, Dec 2016.
[51] S. Gezici and Z. Sahinoglu, "Ranging in a single-input multiple-output (SIMO) system," *IEEE Communications Letters*, vol. 12, no. 3, pp. 197–199, Mar. 2008.

Musa Furkan Keskin received the B.S. and M.S. degrees from the Department of Electrical and Electronics Engineering, Bilkent University, Ankara, Turkey, in 2010 and 2012, respectively. He is currently working towards the Ph.D. degree at the same department. His current research interests include signal processing, wireless localization, and visible light communications.

Sinan Gezici (S'03–M'06–SM'11) received the B.S. degree from Bilkent University, Turkey in 2001, and the Ph.D. degree in Electrical Engineering from Princeton University in 2006. From 2006 to 2007, he worked at Mitsubishi Electric Research Laboratories, Cambridge, MA. Since 2007, he has been with the Department of Electrical and Electronics Engineering at Bilkent University, where he is currently a Professor. Dr. Gezici's research interests are in the areas of detection and estimation theory, wireless communications, localization systems, and visible light communications. Among his publications in these areas is the book Ultra-wideband Positioning Systems: Theoretical Limits, Ranging Algorithms, and Protocols (Cambridge University Press, 2008). Dr. Gezici has been an associate editor for IEEE Transactions on Communications and IEEE Wireless Communications Letters.

Orhan Arikan was born in 1964, in Manisa, Turkey. In 1986, he received the Bs.C. degree in Electrical and Electronics Engineering from the Middle East Technical University, Ankara, Turkey. He received both the M.S. and Ph.D. degrees in Electrical and Computer Engineering from the University of Illinois Urbana-Champaign, in 1988 and 1990, respectively. Following his graduate studies, he worked for three years as a Research Scientist at Schlumberger-Doll Research Center, Ridgefield, CT, USA. During this time, he was involved in the inverse problems and fusion of multiple modality measurements. In 1993, he joined Electrical and Electronics Engineering Department of Bilkent University, Ankara, Turkey. His research interests are in the areas of statistical signal processing and remote sensing. Currently he is a professor and the Chairman of the Department. In 1998, He received the Distinguished Teaching Award of Bilkent University. In 2002, He received the Young Investigator Award in Engineering from Turkish Scientific and Technical Research Foundation. He has served as the Chairman of IEEE Signal Processing Society, Turkey Section in 1995-1996 and served as the President of IEEE Turkey Section in 2000-2001.